Scientific African 23 (2024) e02042

Contents lists available at ScienceDirect

Scientific African

journal homepage: www.elsevier.com/locate/sciaf

Modeling of soil erosion risk in a typical tropical savannah landscape

Mawuli Asempah [a,*], Christopher Allan Shisanya [b], Brigitta Schütt [a]

[a] Department of Earth Sciences, Institute of Geographical Sciences, Freie Universität Berlin, Malteserstraße74-100, Berlin 12449, Federal Republic of Germany

[b] Department of Geography, Kenyatta University, P.O. Box 43844, GPO, Nairobi 00100, Kenya

ARTICLE INFO

Editor: DR B Gyampoh

Keywords:
Erosion risk prediction
Potential erosion risk
RUSLE model
Soil degradation
Soil erosion damage

ABSTRACT

Tropical savannah landscapes are faced with high soil degradation due to climate change and variability coupled with anthropogenic factors. However, the spatiotemporal dynamics of this is not sufficiently understood particularly, in the tropical savannah contexts. Using the Wa municipality of Ghana as a case, we applied the Revised Universal Soil Loss Equation (RUSLE) model to predict the potential and actual soil erosion risk for 1990 and 2020. Rainfall, soil, topography and land cover data were used as the input parameters. The rate of predicted potential erosion was in the range of 0–111 t $ha^{-1}yr^{-1}$ and 0–83 t $ha^{-1}yr^{-1}$ for the years 1990 and 2020, respectively. The prediction for the rate of potential soil erosion risk was generally higher than the actual estimated soil erosion risk which ranges from 0 to 59 t $ha^{-1}yr^{-1}$ in 1990 and 0 to 58 t $ha^{-1}yr^{-1}$ in 2020. The open savannah areas accounted for 75.8 % and 73.2 % of the total soil loss in 1990 and 2020, respectively. The validity of the result was tested using *in situ* data from a 2 km^2 each of closed savannah, open savannah and settlement area. By statistical correlation, the predicted soil erosion risk by the model corresponds to the spatial extent of erosion damages measured in the selected area for the validation. Primarily, areas with steep slopes, particularly within settlement, were identified to have the highest erosion risk. These findings underscore the importance of vegetation cover and effective management practices in preventing soil erosion. The results are useful for inferences towards the development and implementation of sustainable soil conservation practice in landscapes with similar attributes.

Introduction

Soil erosion is influenced by natural factors such as rainfall, topography as well as soil physical and chemical characteristic coupled with anthropogenic activities [1,2]. The anthropogenic influence of soil erosion include land modification through agriculture, deforestation, construction and general land use [3]. Soil erosion results in on-site losses of fines and dense particles, such as clay and humus, that are essential soil nutrients carriers and also function as soil stabilising agents [4]. Soil erosion potentials are high within subhumid and dry-subhumid tropics given the high rainfall intensities and amount prevalent in such regions [5,6]. Besides rainfall, soil erosion within the tropical regions are generally concentrated in space over time (e.g. during change in cropping systems such as crop rotation) [7]. The consequential effects are multi-faceted, and include decreasing crop yields and water resource degradation, which

* Corresponding author.
E-mail address: mawuli.asempah@fu-berlin.de (M. Asempah).

https://doi.org/10.1016/j.sciaf.2023.e02042
Received 12 July 2023; Received in revised form 22 November 2023; Accepted 19 December 2023
Available online 21 December 2023

are observed in high turbidity and particle-induced pollutants. The water holding capacity of reservoir is reduced through sedimentation thereby altering the hydrological regimes, and further compounding flood risk as a result of riverbed filling and stream plugging [8–10].

Globally, soil erosion disrupts sustainable functioning of ecosystems [11]. The impacts of soil erosion jeopardise the potential of a variety of ecosystem services, which could be derived from healthy soil. The Millenium Ecosystem Assessment [10] points out that ecosystem services for soil erosion control are on the decline globally. Globally, the range of soil erosion is highly substantial [12] and threatens ecological integrity, biodiversity and future agriculture productivity [13]. According to Ref. [4] about 1094×10^6 hectares - corresponding to c. 8.4 % of global land surface - are affected by soil erosion by water, with 751×10^6 hectares (5.8 %) even severely affected by water erosion. In contrast, wind-induced soil erosion affected about 549×10^6 hectares (4.2 %) of the world's land mass, with about 296×10^6 hectares (2.3 %) being severe [14]. Economically, the impact of the deterioration of arable land amounts to billions of dollars [15]. According to Ref. [16], Africa faces irreversible soil productivity losses due to water erosion at national scales; in some parts of sub-Saharan-Africa already about 20 % of crop yield has been permanently reduced due to soil erosion processes. Obalum et al. [17] postulate for subsahara Africa about 50 % of productivity losses, which are attributable to soil erosion processes. In East Africa region [18] modelled land susceptibility to water and wind erosion risks and established a 10 % moderate or elevated water erosion risks (>10 t $ha^{-1}yr^{-1}$) while prediction for wind erosion was 25 % moderate or elevated erosion. Similarly, [19] predicted 19.5 % of high to very high erosion risk in West Africa following a regional erosion risk mapping. In Ghana, the impact of soil erosion has been felt since the early 1930s [16]. Research has shown that since that time about 29.5 % of the country's erosion impact could be classified as slight-to-moderate sheet erosion, with 23 % being severe sheet and gully erosion, and 43.3 % being classified as high sheet and gully erosion [20]. However, it is anticipated that actual figures may be significantly higher owing to enormous strain on land due to a mix of physical and socioeconomic reasons, including population pressure, poor farming methods, and effects of global climate change [21].

The trend of soil erosion implies a great threat to food security, poverty reduction and biodiversity conservation which are core component of the United Nations sustainable Development goals (SDGs). While SDG 15 aimed at protecting, restoring and promoting sustainable use of terrestrial ecosystem as well as halting and reversing land degradation and biodiversity loss, the SDGs 1 and 2 seek to end poverty and hunger, respectively [22]. Aside the destruction of ecosystem and loss of biodiversity, Soil erosion reduces the fertility and productivity of the soil leading to low agricultural productivity. Soil erosion risk modelling is part of efforts to promote sustainable agriculture, water and biodiversity conservation which are vital to achieve the SDGs [22]. Assessing soil erosion risk is therefore a step towards planning sustainable conservation practices in the face of climate variability and land use intensification for the realization of the aforementioned global goals [23]. Several empirical, statistical, and physical models are applicable in estimating soil erosion risk [24–27]. Generally, the selection of a model is highly dependent on the availability of a data, its applicability to study area's attributes, intended use, processes and the calibration needs [28,29]. In practice, the Universal Soil Loss Equation (USLE) is one of the widely used empirical models[30]. Also, its derivatives, the Revised Universal Soil Loss Equation (RUSLE) [31], the Water Evaluation and Planning (WEAP), the Soil and Water Assessment Tool (SWAT) [32] and the Water Erosion Prediction Project (WEPP) [33] have been extensively explored to model erosion risk under various contexts, including different climatic and soil conditions as well as land use practices.

In this study, Wa municipality, an area typical for the tropical savannah agro-ecological zone, remote sensing techniques and data processing with Geographic Information Systems (GIS) build the basis for soil erosion risk modelling applying the RUSLE. GIS was applied in extracting, delineating and manipulating land characteristics that serve as input parameters for the estimation of soil erosion risk by the RUSLE model [34–36]. The RUSLE model which was initially developed for plot-based experiments has been applied for modelling at macro-scale and is useful for identifying areas which are vulnerable to soil erosion [37–39]. However, the means of validating the RUSLE model's result is lacking. This study provides a three-stage approach to better estimate the soil erosion risk by predicting the potential soil erosion risk, the actual soil erosion risk and testing the validity of the results using soil erosion damage data that was measured in the field. In order to understand within the vulnerable savannah agro-ecological zone, the relevant dynamics of soil erosion across time, this case study on Wa municipality models the spatial pattern of soil erosion risk as well as potential erosion for the years 1990 and 2020 owing to changes in climate patterns and land use and land cover over these periods. Thus, the study evaluates how changes in land use and land cover (LULC) influence soil erosion risk in Wa municipality through the analysis of temporal soil erosion estimates. First, we modelled potential erosion for the Wa municipality, and predicted the actual soil erosion risk for the year 1990 and 2020 using the RUSLE model. We then validated the modelled soil erosion risk using field measurements. This approach, especially the validation option, is useful, applicable and provided the basis for making inferences in future studies especially in the tropical context.

Materials and methods

Study area

Wa municipality is situated in Ghana's Upper West Region, (between 10° 14′ 46.32″ N and 09° 42′ 5.04″ N and 02° 33′ 14.04 W and 02° 0′ 57.96″ W). According to the 2010 census, 102,214 people reside in the municipality's 579 km^2 land [40]. According to the Ghana population and housing census for the 2021 census, the municipality's population has grown to 200,672 people, of which 143,358 people (71.4 %) live in urban areas while 57,314 of people (28.6 %) are residing in rural areas [41].To the western border of the study municipality lies the Wa West administrative District of Ghana, with the Nadowli administrative district lying to the east. In the Guinea Savannah agro-ecological zone, the Wa Municipal District (Fig. 1) is characterised by flora that has adapted to drought.

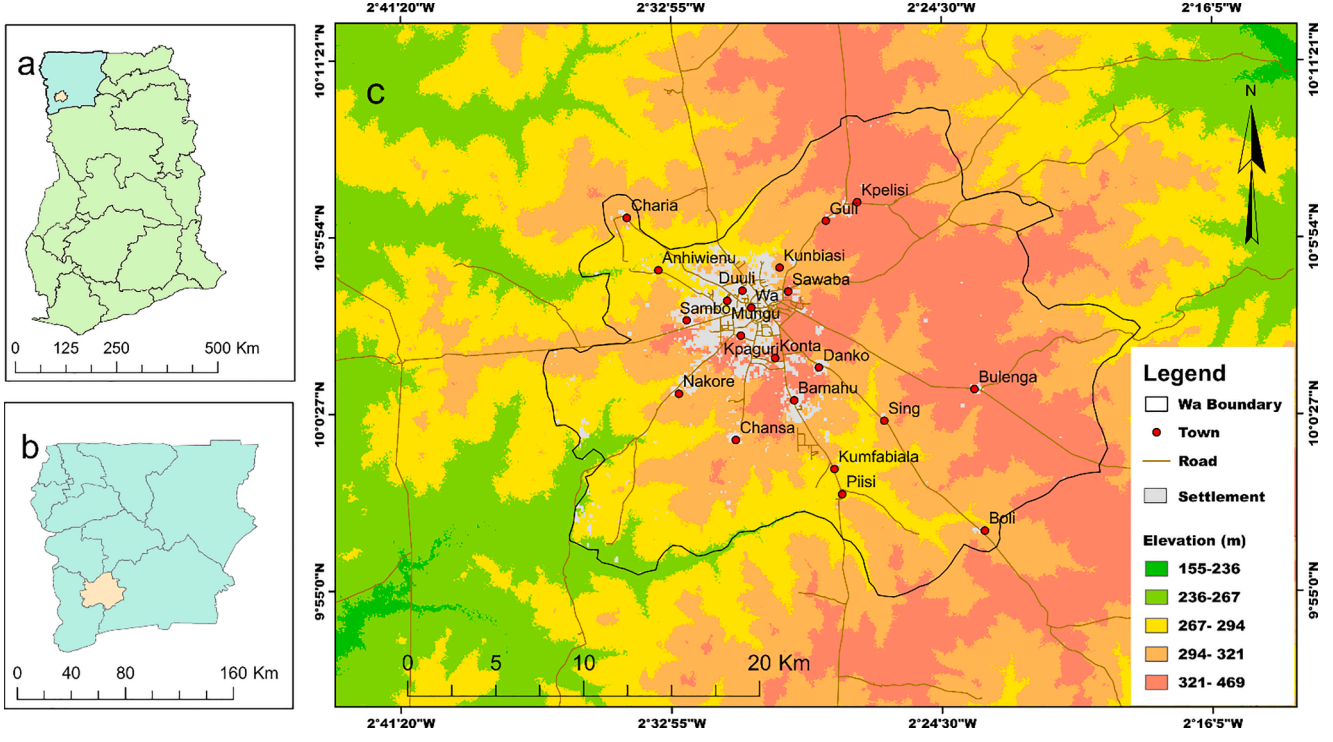

Fig. 1. Map of Wa municipality's land elevation within the context of the Upper West region of Ghana. (a) A map of Ghana displaying its sixteen administrative regions, with Upper West shaded. (b) Map of the Upper West region displaying the eleven administrative districts and their borders; Wa municipality is shown by shade. (c) Digital elevation model (DEM); the black line designates the Wa municipality's administrative boundary. Data source: See Shuttle Radar Topography Mission (SRTM) DEM, obtained from United States Geological Survey's (USGS) Earth Explorer database. Retrieved from https://earthexplorer.usgs.gov/ on 18 September 2020).

A savannah landscape characterizes the Wa municipality. Its relief is slightly undulating in the savannah high plains, which are located between 160 and 300 m a.s.l. The southern and the northern areas are low-lying and constitute two drainage systems within the municipality with the main drainage system in the north. The main soil types are laterites, which can be found across the entire municipality, but in its western part shallow savannah ochrosols predominate. Locally clayey and sandy textures predominate; especially Nakore township and its environ in the western part of the municipality has abundant occurrence of sandy materials, while the community of Charia township and its environ is well known for a predominance of clay. Rivers in the low-lying areas are periodical and provide discharge during the rainy season. The valleys also form the two principal drainage systems in the Wa municipality. The Billi and its tributaries drain the northern part of the Wa municipality, the Sing-Bakpong and its tributaries drain the southern part [42],both are tributary to Black Volta River.

Climate of Wa municipality is tropical and characterised by two distinct seasons as controlled by the dry Northeast trade winds (which originate from the sub-tropical high-pressure region) and the South-west monsoon winds (which originate from the Indian subcontinent in south-westerly direction). The wet season, which runs from May to September, is linked to the southwest monsoon winds [42,43]. The dry Harmattan season usually commences in November and last till around March and is caused by the northeast trade winds. The mean annual temperature ranges from 20.5 to 37.2 °C, seldom drops below 15.5 °C and occasionally might exceed 40 °C. The relative humidity ranges from 68 to 72 %, with the mean annual rainfall varying between 840 and 1400 mm within the 1990–2020 period [42,44]. Under the influence of Harmattan winds, relative humidity can drop below 20 % during extended drought periods.

The central part of Wa municipality is highly urbanized with cluster of towns which significantly expanded since 1990 [45]. The northern part of the municipality is an expansion of rural settlements such as the Charia, Guuli and Anhiwienu, with these areas lying in the low-lands close to the major rivers in the region. Piisi, Boli and Sing villages are located in the slightly undulating low lands south of Wa; also, their location is close to the major rivers. In contrast, Nakore and Bulenga villages are located in the headwater areas. All these smaller villages correspond to nucleated villages and are directly connected by roads to Wa; between the villages along the roads dispersed settlements occur. The remaining area is predominantly rural and characterized with savannah vegetation. Agriculture and further processing of agricultural products characterizes the economic structure of Wa municipality [42]. Major crops cultivated are millet, sorghum, yam, soya beans and groundnuts. Beyond, trees of economic value such as the baobab, the shea tree, the teak tree among others are widespread in the area, and serve to diversify agricultural products and thus sustain livelihood and development [46, 47]. Seasonal bushfires, climate change, and expanding built-up regions strain economic trees' advantages and livelihoods. Based on the general characteristic of the municipality coupled with rapid settlement expansion and exposure of the landscape due to anthropogenic activities, the tendency for soil erosion risk in the area is high.

RUSLE model

We applied the RUSLE model in estimating the average annual rate of soil loss based on the sheet and rill erosion forms, and to show the distribution of potential and predicted soil erosion risks across space in the Wa municipality. The RUSLE model's comparative advantage in modelling data scarce landscapes owing to its flexible data requirements make it applicable to the Wa municipality other than physically distributed models with extensive data requirement [37]. We applied the ArcGIS in conjunction with QGIS and the machine learning programme R to process the raster-based input data required to implement the RUSLE model. Estimation soil erosion risk was conducted applying the formula [31]:

$$A_{SE}\left[\text{t ha}^{-1}\text{yr}^{-1}\right] = \text{R} \times \text{K} \times \text{L S} \times \text{C} \times \text{P} \tag{1}$$

where:

A_{SE} connotes the average soil erosion rate per annum (t ha^{-1} yr^{-1}); *R* connotes rainfall erosivity factor (R-factor) (MJ mm ha^{-1} h^{-1} yr^{-1}); *K* connotes soil erodibility factor (K-factor) (t h MJ^{-1} mm^{-1}); LS represents the slope length and steepness factor (LS-factor); C represents the cover management factor (C-factor), and *P* connoted the conservation support practice factor (P-factor). Weighted value 0 and 1 are the respective lower and upper limits of C and *P* values, and this is influenced by the level of vegetation and conservation management practices available on the landscape.

To better explain the effects of land use change on morphodynamics, we applied Eq. (1) and did set the C-factor and P-factor value to 1 as the identity number for multiplication operations. We define the resulting average potential soil erosion rate per annum A_{pot} (t ha^{-1} yr^{-1}) as the soil loss of a land surface without conservation and management practice.

Data from diverse sources were used for the computation of the input variables for the model (Table SM1). The K-factor was generated using soil grid data from the International Soil Reference Information Centre (ISRIC) database (See https://soilgrids.org). A trapezoidal rule approach was complemented with machine learning for an onward computation to generate the K-factor input parameter. The LS-factor is obtained from the SRTM DEM with a horizontal resolution of 30 × 30 m. C-factors were deduced on the terrain cover characteristic presented in the Wa municipality's LULC classification for the years 1990 and 2020 [45]. All the input raster data were of 30 × 30 m horizontal resolution except for the K-factor raster data that was available in 250 × 250 m resolution. By employing nearest neighbor techniques, the K-factor raster was resampled to the same resolution and projection to ensure model accuracy.

Soil Erodibility factor (K). The K-factor, ((t ha h)*(ha MJ mm)$^{-1}$) defines the proneness of soil to erosion as a result of the soil's inherent properties that influence the resistance to detachment. Soil physical properties (including porosity, structure and texture) play significant roles in soil erosion as they influence the degree of resistance or susceptibility to rainfall impacts in the form of splash or overland flow [48]. In computing the soil erodibility factor, we obtained data from the ISRIC database. The soil information applied

in estimating the K-factor with the equation proposed by Sharpley & Williams in 1990, wich includes contents of silt, clay, sand and organic matter. While these data are at the "SoilGrids" and available for soil layers from 0 cm to 200 cm depth (with other sub divisions), we used weighted averages of these characters for the soil layers within 0–30 cm depth. By employing numerical integration through a Trapezoidal equation, the average values for each layer of overall depth intervals for 0–30 cm were estimated using a weighted mean of the predictions in the interval [49]:

$$\frac{1}{b-a}\int_{a}^{b} f(x)dx \approx \frac{1}{(b-a)}\frac{1}{2}\sum_{K=1}^{N-1}(X_K+1-X_K)(f(X_K)+f(X_K+1)) \tag{2}$$

where:

N connotes the number of depths; xk represents the *k*th depth; f(*xk*) is the estimated value of the target variable (i.e., soil property) at depth *xk*.

Machine learning was employed in the processing and generating of the weighted averages of the respective raster layers for the various soil properties as inferred from Eq. (2). The output raster layers were used subsequently as the input parameters for the computation of the K-factor using the proposed Eq. (3) [50,51]:

$$k = 0.1317\left(0.2+0.3*e^{\left\{-0.0256SAN\left(1-\frac{SIL}{100}\right)\right\}}*\left(\frac{SIL}{CLA+SIL}\right)^{0.3}\right)*\left\{1-\frac{0.25*TOC}{TOC+e^{(3.72-2.95*TOC)}}\right\}*\left\{1-\frac{0.7*SN1}{SN1+\ e^{(22.9*SN1-5.51)}}\right\} \tag{3}$$

where:

SAN represents sand, SIL connotes silt, CLA is clay, and C represents the organic carbon contents of the soil (mass-%) and SN1=1-SAN/100.

Slope Length and Steepness factor (LS). LS-factor is an important parameter that influences soil erosion, and it represents the cumulated effects of slope steepness (S) and slope length (L) on soil erosion [52]. The distance between an upslope starting point to downslope point where soil deposition starts is referred to as the slope length (L) [53]. The exposure to soil loss is increased by increasing the length of the slope and the steepness per unit area, which increases the values of runoff and associated flow velocity [54]. A steeper slope has a higher tendency to influence erosion because it produces higher flow velocity of runoff, thereby increasing the shear stress on the surface and in consequence mobilising more material [55]. The combined effects of the slope length and the steepness measure the topographic impact on erosion [54–56]. The LS-factor utilised in the RUSLE model was derived from a 30 × 30 m resolution SRTM DEM by computation using the Hydrology module [53] of the SAGA GIS software. The fill sink algorithm was used for data pre-processing, utilising the spill-elevation method [57]. The DEM was further processed by applying the multiple flow direction tool (MFD) [58] in SAGA GIS for the attribution of flow directions and accumulation [59]. The computation of LS-factor considers unit contributing area that is factored distribution of LS-factor over the entire landscape [60].

Rainfall erosivity factor (R). The *R*-factor is the capacity of rain to triggger soil erosion [53,61]. The Rainfall variables that determine the total erosivity includes the drop size and drop distribution, amount and intensity coupled with terminal velocity [62,63]. The raindrop impact partly determines the rate of runoff usually associated with rain and, in effect, reflects in numerical value of rainfall erosivity [30]. Based on high-resolution data, a product of long-term average rainfall energy (E) together with a maximum of 30 min rainfall intensity (I30) for storm events is desirable for computation of Rainfall erosivity. However, in absence of high-resolution and sufficient data, several context-specific simplified approaches have been proposed to estimate an R-factor [64,65]. In this study, we explored tropical landscape-specific equations applicable to the context of Wa municipality in computing R-factor (in MJ mm ha^{-1} $h\text{-}^{1}$ yr^{-1}). The equation for estimating R [66] is given as follows:

$$\mathrm{R} = 0.562(\mathrm{Ar}) - 8.12 \tag{4}$$

where:

R denotes Rainfall erosivity factor, and (Ar) denotes average annual rainfall.

Time series erosivity was computed from the long-term rainfall data from 1980 to 1990 and 2010–2020 for the examined years 1990 and 2020, respectively. The inverse distance weighted (IDW) technique was used to interpolate the long-term rainfall data. The

Table 1
Classes of Land Cover and their spatial extent (%) in the Wa municipality area. For the C-factor values assigned for the respective land cover classes and references are provided.

	Area Covered (%)			
Land cover classes	1990	2020	Weighted C-factor value	Source of Weighted C-factor value
Closed savannah	22.22	15.77	0.001	[74,75]
Open savannah	70.30	67.72	0.002	[76]
Other (bare land)	3.83	3.82	1	[77,78]
Settlement	1.28	10.33	0.8	[77]
Vegetated wetland	2.30	2.16	0.21	[77]
Water	0.07	0.20	0	[77,78]

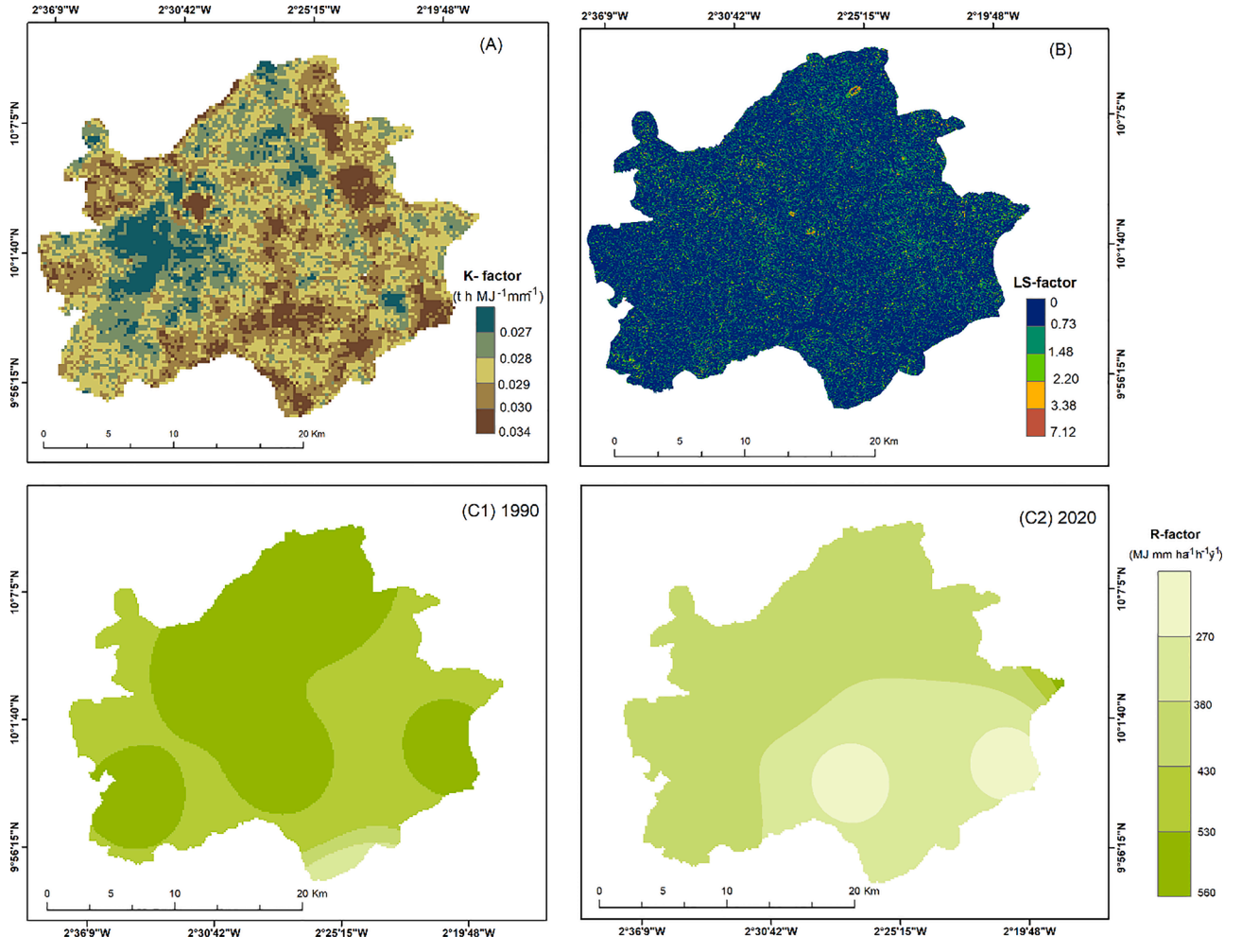

Fig. 2. Map of K, LS and R-factor. (A) Soil erodibility map for the Wa municipality (Data source: ISRIC- World Soil Information "SoilGrids" provides a raster (TIF format) global soil map and associated information (See https://soilgrids.org; accessed on 20 September 2021). (B) LS factor map for the Wa municipality. Source of Data: SRTM DEM from USGS' Earth Explorer website (See https://earthexplorer.usgs.gov/ 15th September 2020). (C1) The R-factor for 1990 (C2) the R- factor for 2020 (See data base at: https://power.larc.nasa.gov/ accessed on 15 April 2021).

output raster of the interpolation was extracted to the extent of the study area and subsequently applied in Eq. (4) to compute the erosivity factor.

Land Cover and Management Factor (C). The C-factor is explained as the influence of vegetation cover on erosion [67]. Barelands are more prone to erosion than vegetated lands as – among others - they are protected to rain drop impact by leave coverage, as soil cohesion is supported by plant roots and as vegetation increases surface roughness and, thus, decelerates flow velocity [30,68,69]. Therefore, depletion in vegetation cover may cause the C-factor to increase significantly, and in effect increase in soil loss rate. The C-factor corresponds to an assigned numeric value (0–1), which is based on the land cover types and their resistance capability to erosivity capabilities as presented as vegetative protection (Table 1). Completely bare land has a C-factor of 1, while densely vegetated land that tends to protect the soil from detachment has a C-factor of 0. Hence, the lower the C-factor value the better erosion prevention capability and vice versa [68]. Several approaches are proposed for computation of C-factor. The approach of Benkobi et al. (1994); also [31] is based on a field experiment that considers the C-factor as the product of soil loss ratio and the total storm energy of a rainfall event with 30 min intensity (*EIn*) divided by the total storm erosivity *EI*. The soil loss ratio is computed as the product before land use, surface cover, canopy cover, soil moisture and surface roughness [31,71]. Though this approach seems preferable, some limitations hinder its adoption. The approach involves a laborious field experiment to obtain the surface cover, canopy cover, soil moisture and surface roughness on the assumption of their uniform distribution throughout the entire landscape [72]. The samples obtained may not reflect exact prevailing conditions of the entire landscape and may differ from season to season [31,72]. Base on this we employed the option of satellite images which gives a better impression about the landscape characteristics in terms the type and extent of vegetation coverage.

The C-factor was deduced from a supervised LULC classification to establish the type as well as the stretch of land cover and by this to achieve a reliable C-factor as input parameter for the RUSLE model (Table 1). We used LULC maps for the years 1990 and 2020 generated from satellite images adapted from Ref. [45] (Fig. 3). The categorization and definition of LULC classes (Table SM 2) was adapted after Ghana's LULC classification scheme to visualize remote sensing data [73]. Based on the land use and land cover classes, we estimated the C-factor by assigning weighted C-factor value to each land use and land cover types. The weighted value of each land use and land cover types were carefully selected by evaluating literature in the context of tropical savannah landscape ([69–73]. The C-factor raster images that served an input parameter for the RUSLE model was obtained by multiplying the established weighted value for each LULC class to their corresponding weighted C-factor value (Table 1).

Conservation Support Practice factor (P). P-factor values ranges from 0 to 1 and indicate the effectiveness of conservation practices in the landscape as a measure against soil erosion [79,80]. A lower P-factor value implies better management and conservation practices and higher effectiveness in reducing soil erosion. In comparison, a high P-factor value represents less effective conservation practices and less effective erosion control ability [81]. Thus, a P-factor value of 0 indicates highest erosion control ability, while a P-factor value of 1 means no soil conservation or erosion control measure is implemented [79,82]. The type of conservation and management option highly depends on the topography of landscape; hence computation of P-factor considers slope of landscape to adopt conservation activities such as contour plowing, strip cropping and terrace risers and bunds to control surface runoff and force infiltration [81,83].

Field survey of on-site erosion damages

To validate the results of RUSLE model, we conducted in January/February 2022 a field survey to measure the spatial extents of on-site soil erosion damages, specifically, rills and inter-rills in the Wa municipality. Specifically, a survey was implemented on 2 km^2 plots each in the Wa municipality's closed savannah, open savannah, and settlement LULC areas. On-site damages that qualify as rills and inter-rill in the context of the RUSLE model specification for soil erosion risk assessment were identified, mapped and measured [84]. A potable GPS (Garmin 60Cx) was used in mapping and geocoding the individual damage spots that comprise linear channels whose dimensions are within rill and inter-rills categories other than ephemeral gullies and gullies [85]. Rills as linear erosion channels had a cross-sectional area of less than 929 cm^2 and a maximum depth of 0.5 m [85,86]. The spatial extent of damages from various survey plots was categorised into five classes of damages in a digitised damage map depicting extent of disturbance within each LULC area (Fig. 5) and systematically and statistically compared to the corresponding soil erosion risk predicted by the RUSLE model. Prior to the systematic and statistical comparison, the data was standardized by logistic transformation.

Results

RUSLE model input parameters

Soil Erodibility factor (K). Within this model, the K-factor values estimated for the whole landscape of Wa municipality ranges from 0.024 to 0.034 t h MJ^{-1} mm^{-1}, with the mean value corresponding to 0.029 t h MJ^{-1} mm^{-1} (std.=0.001) (Fig. 2A). The values spread heterogeneously across the study municipality with relatively low values (0.024–0.028 t h MJ^{-1} mm^{-1}) in the western and south-western part of the municipality where coarse-textured soils predominate. In the most western part of Wa municipality K-factor values of 0.029–0.030 t h MJ^{-1} mm^{-1} can be observed. Isolated patches of highest K-factor values occur across the entire study area. The field survey showed a distribution of diverse soil characteristics, corresponding to the diversity in k-factor for the area.

Slope Length and Steepness factor (LS). In the study municipality, the LS-factor values range from 0 to 7.12, with a mean value of 2.96 (std = 0.06) (Fig. 2B). Due to the overall slightly undulating terrain in the Wa municipality LS values remain < 2.2. Correspondingly, variability of the LS-factor is low. Steep slopes and coinciding increased LS-factors predominantly occur around the central and north-eastern areas of the municipality. Locally slopy areas also occur in the urbanized of Kpelisi, Mungu, Duuli and the Wa township.

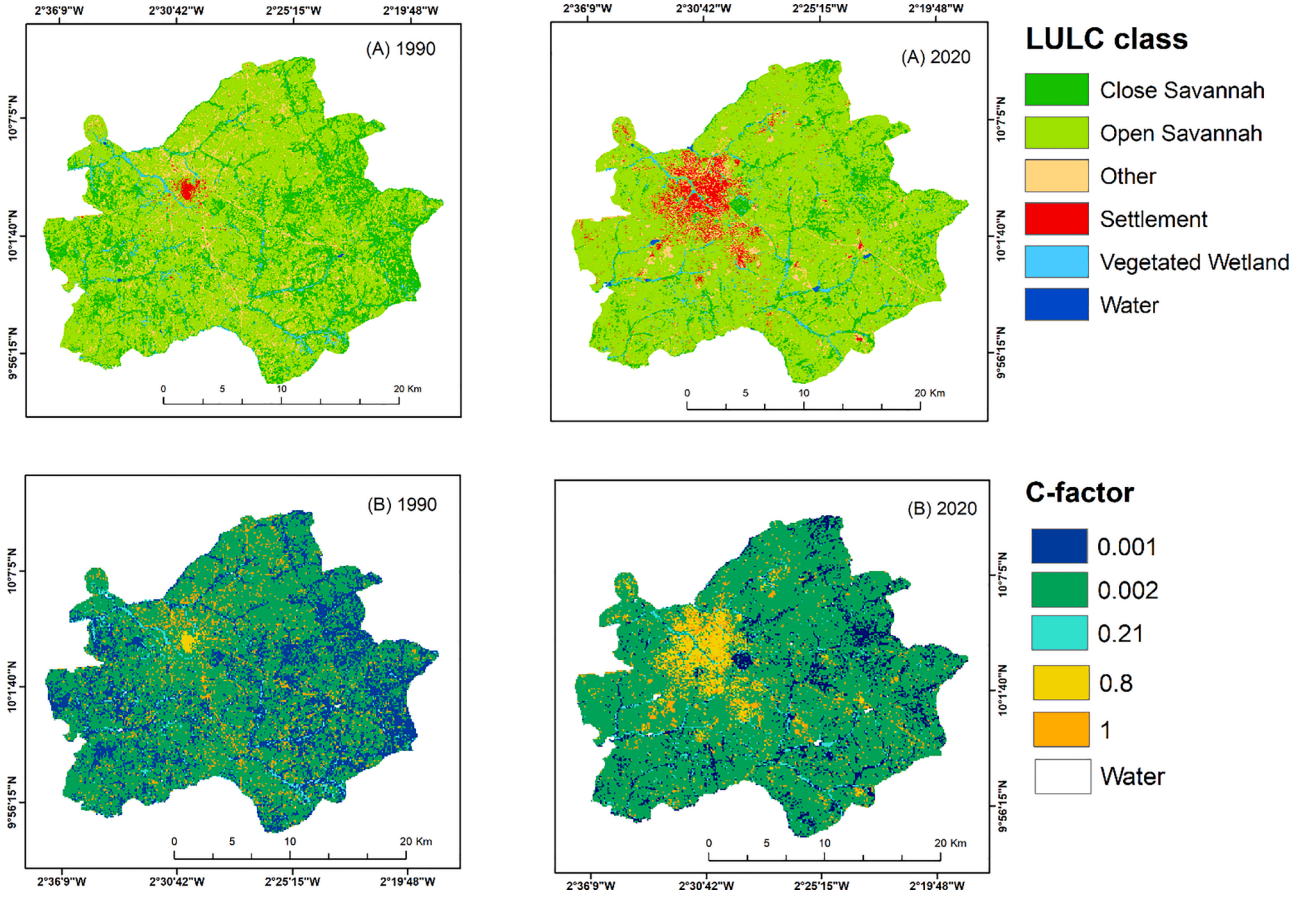

Fig. 3. LULC map for the Wa municipality and corresponding C-factor input parameter for modelling soil erosion risk for the years 1990 and 2020. (A) 1990 and (A) 2020 are LULC maps for 1990 and 2020, respectively, while (B) 1990 and (B) 2020 are corresponding C-factor input parameters for the years 1990 and 2020, respectively (LULC classification adapted from Ref. [45]).

Rainfall erosivity factor (R). The decadal rainfall for the entire Wa municipality from 1980 to 1990 averaged 948 mm (std.=0.74) with a corresponding average R-factor of 524.83 MJ mm ha^{-1} h^{-1} yr^{-1} (std.=0.53). In the year 2020 rainfall averaged 723 mm, also with a corresponding R- factor of 398.63 MJ mm ha^{-1} h^{-1} yr^{-1}. This data is consistent with Ghana meteorological agency and Ghana statistical service's annual rainfall statistics for the Wa municipality [42]. Generally, rainfall erosivity factors (R) differ in spatial variability across the Wa municipality for the observation years 1990 and 2020. In 1990, the highest R-factors ranging between 530 and 560 MJ mm ha^{-1} h^{-1} yr^{-1} occurred along a N-S corridor across Wa municipality, while in the neighboring areas R-factors varied between 480 and 530 MJ mm ha^{-1} h^{-1} yr^{-1} (Fig. 2 C1). In contrast, during the study year 2020 the R-factor is evenly distributed across the study area with values predominantly < 480 MJ mm ha^{-1} h^{-1} yr^{-1}. (Fig. 2 C2).

Estimated Cover factor (C) and Support Practice factor (P). The area of Wa municipality is predominantly covered with the savannah open vegetation that constitutes the arable land for various agricultural activities. Settlement and bare lands areas show the highest C-factor values (0.8 and 1, respectively) (Fig. 3). The smallest C-factor values are assigned to areas with dense vegetation cover (example the closed savannah vegetation and the vegetated wetland areas). While the closed savannah areas are characterised by a dense cover of trees and bushes and a dense ground vegetation layer, the vegetated wetlands areas are characterised by a dense grass and shrub cover that get inundated regularly. Due to the expansion of settlement areas and corresponding decline of savannah areas between 1990 and 2020, the area characterized by low C-factor values is distinctly larger in the year 1990 than in the year 2020, as it is also evident in the LULC classification (Table 1). Previous scientific works extensively established P-factor values in the context of typical tropical regions. However, our field survey shows that support or erosion control practices is lacking in the Wa municipality; thus, our model considered 1 as the value for the P-factor.

Estimated potential erosion risk A_{pot}

The modelled potential erosion risk for the years 1990 and 2020 is expressed as soil loss by potential erosion $A_{pot.}$ and focusses on the physical factors controlling erosion, thus, exclusively the R, LS and K-factors are taken as input for the RUSLE model. The resulting maps of potential erosion risk (Fig. SM1) are complemented by the corresponding statistical values (Table 2) for the respective years. Altogether, for 1990 the estimated rate of potential erosion range between 0 and 111 t $ha^{-1}y^{-1}$ corresponding to a total potential soil loss in Wa municipality of c. 395,959 tons. For the year 2020 the rate of potential erosion is estimated to lie within 0–83 t $ha^{-1}y^{-1}$, with a corresponding total potential soil loss in Wa municipality of c. 376,266 tons. For both observation years more than 50 % of the landscape was prone to high-to-extreme grades of potential erosion risk. For 1990 36.5 % of the Wa municipality was exposed to a high potential erosion risk; within the error margins this equals the area being exposed to high potential erosion in 2020 (38.1 %; Table 2). Areas with "low" and "moderate" potential erosion risk predominantly occured in flat areas. In contrast, areas exposed to the "very high" and "extreme" potential erosion risk corresponded to areas with high LS-factors or occurred in urbanised areas with extensive road networks and.

Estimated soil erosion risk

In 1990, about 83.9 % of the Wa municipality were exposed to low to a moderate soil erosion risk while in 2020 spatial extent of areas exposed to low to moderate soil erosion risk decreased to 76.0 % (Table 3). These areas of low to moderate soil erosion risk contributed in 1990 to 44.8 % of the total erosion in Wa municipality, for 2020 this value amounted 39.3 %. In contrast, areas that were exposed to "high" and "very high" soil erosion risk covered in 1990 15.35 % of the area of Wa municipality, and increased in spatial extent to 23.4 % in 2020; it is estimated that these areas exposed to "high" and "very high" soil erosion risk contributed about half of the municipality's total soil loss in the respective year. The statistics document the contribution of the different soil erosion risk grades to the estimated annual soil loss: For 1990 total soil loss in Wa municipality is estimated 150,401 tons increased to an estimated total erosion of 200,464 tons in 2020. The soil erosion risk in Wa municipality averaged in 1990 2.6 t ha^{-1} y^{-1} (range of spatial distribution: 0–59 t ha^{-1} y^{-1}) and in 2020 3.5 t ha^{-1} y^{-1} (range of spatial distribution:0–68 t ha^{-1} y^{-1}) (Fig. 4). Exposure to high soil erosion risk especially occurred around the central part of the Wa municipality, with isolated patches of very high and severe soil erosion risk. Very high to extreme soil erosion risk predominantly can be observed at hillside locations within settlement areas; this observation applies for both observation years.

Spatial variations in soil erosion risk for Wa municipality closely correlate to land use. In general, the areas covered by open

Table 2
Estimated soil loss by potential erosion $A_{pot.}$ at Wa municipality by different severity classes.

		1990: Soil loss by potential erosion $A_{pot.}$				2020: Soil loss by potential erosion $A_{pot.}$			
Potential Erosion Risk	Soil erosion (t $ha^{-1}y^{-1}$)	Total area (ha)	Total area (%)	Total soil loss (t y^{-1})	Total soil loss (%)	Total area (ha)	Total area (%)	Total soil loss (t y^{-1})	Total soil loss (%)
Low	<3	16,933.8	29.3	34,352.6	8.7	15,933.9	27.6	28,840.3	7.7
Moderate	3–5	8101.2	14.0	42,541.4	10.7	7050.2	12.2	27,495.6	7.3
High	6–10	21,119.0	36.5	145,261.1	36.7	22,019.0	38.1	147,747.8	39.3
Very High	11–15	8223.4	14.2	105,664.4	26.7	8519.3	14.7	104,957.9	27.9
Extreme	>15	3506.6	6.1	68,139.9	17.2	4306.5	7.5	67,224.5	17.9
		57,884	100.0	395,959.4	100.0	57,828.9	100.0	376,266.1	100.0

Table 3
Estimated soil loss by soil erosion A_{SE} and soil erosion risk at Wa municipality by different severity classes.

		1990: Soil erosion A_{SE} risk by grade				2020: Soil erosion risk A_{SE} by grade			
Soil Erosion Risk	Soil erosion (t $ha^{-1}y^{-1}$)	Total area (ha)	Total area (%)	Total soil loss (t y^{-1})	Total soil loss (%)	Total area (ha)	Total area (%)	Total soil loss (t y^{-1})	Total soil loss (%)
Low	<3	38,166.1	65.9	23,302	15.5	30,002.5	51.9	26,732	13.3
Moderate	3–5	10,421.2	18.0	44,027	29.3	13,960.1	24.10	52,145	26.0
High	6–10	7592.7	13.1	58,751	39.1	10,957.0	18.9	73,729	36.8
Very High	11–15	1288.6	2.2	16,934	11.3	2547.5	4.4	29,811	14.9
Extreme	>15	415.3	0.7	7387	4.9	361.8	0.6	18,047	9.0
		57,883.9	100.0	150,401	100.0	57,828.9	100.0	200,464	100.0

savannah vegetation contribute about three-quarters of the total soil loss in 1990 and 2020 with a spatial extend of open savannah vegetation of 70.4 % in 1990 and 67.8 % in 2020. The areas covered by open savannah vegetation are to a great extent cultivated and grazed, resulting in a high exposure to soil erosion. This is exacerbated by seasonal bush fires that usually occur during Harmattan season that disturb vegetation cover and, thus, expose the area to erosion at the beginning of the rainy season (which advances the harmattan season). Closed savannah vegetation covered in 1990 22.2 % (12,869 ha) of Wa municipality and had shrunk until 2020 to 15.8 % coverage (9134 ha) (Table 4).

Due to the relatively low soil erosion risk under closed savannah vegetation, the decrease in the area covered by the closed savannah vegetation between 1990 and 2020 caused an increased exposure to soil loss in areas covered in 1990 still by the closed savannah. Areas covered by settlements and bareland in general have a high exposure to soil erosion risk [87,88]. The spatial extent of settlement areas in Wa municipality quadruplicated from 5.1 % in 1990 to 22.2 % in 2020. The contribution of areas covered by settlements or barelands to the total soil loss in Wa municipality amounted 13.4 % in 1990 and increased to 20.4 % in 2020 (Table 4).

Validation of modeled soil erosion risk applying RUSLE model

During 2022 field survey in each of the land use classes, closed savannah (Fig. 5A), open savannah (Fig. 5B), and settlement (Fig. 5C), a 2 km^2 test plot was systematically mapped for soil erosion damages. Mapping results were then applied to validate the RUSLE modelling results for soil erosion risk for the year 2020. For each plot area erosion damage maps (Fig. 5 A2, B2, B3) were systematically compared to the 2020 RUSLE modelling results of the soil erosion risk (Fig. 5 A1, B1, C1). Altogether in all three survey plots, 79 linear erosion forms corresponding to rills were mapped and measured. Eighteen (18) of the rills (coverage: 15.1 m^2) were mapped in the closed Savannah vegetation areas, while 26 of the rills (coverage: 69.8 m^2) were mapped in areas covered by open savannah vegetation. In settlement areas degree of on-site damages was highest with a total number of 35 rills mapped (coverage: 109.9 m^2). In total, an area damaged by soil erosion of 194.8 m^2 was mapped within the 6 Km^2 of the three test plot areas.

The extent of on-site damages measured on each of the test plots is consistent with the modelled soil erosion risk for the respective sites. The soil erosion risk for settlement plot (C1) is classified as "high," "very high," and "severe," with a soil loss estimate of 6–54 t ha^{-1} y^{-1}. The areas of high to extreme soil erosion risk correspond to the large spatial extent of soil erosion damages mapped and measured in the settlement test plot (C2). In comparison, in the open savannah vegetation test plot (B1) soil erosion risk is "moderate" to "high" (3–10 t ha^{-1} y^{-1}); the corresponding damage map of the open savannah test plot (B2) shows in comparison to the settlement test plot (C2) comparatively small spatial extent of areas with on-site erosion damages (mostly in the range of 2–5 m^2). Overall, the closed savannah test plot (A1) had the lowest soil erosion risk (< 3 t ha^{-1} y^{-1}). This corresponds to the least spatial extent of all the individual eroded area of less than 3 m^2 in the closed savannah damage map (A2). In a nutshell, for the test plots A1, B1 and C2 estimated soil erosion risk corresponds to the area of on-site damages in the respective test plots A2, B2 and C2.

The moderate to high exposure to soil erosion risk in the open savannah LULC class indicates the high vulnerability of this area. The spatial pattern of the corresponding damage measurements (Fig. 4 B2) is in line with the model results (Fig. 4 B1). The highest exposure to soil erosion was observed in the settlement area plot. The spatial extent of erosion damages (Fig. 5 C2) and the corresponding soil erosion risk map (Fig. 5 C1) underline high exposure to soil erosion. However, spatial accordance of soil erosion damages mapped and soil erosion risk modelled is less solid for the settlement areas than for the areas covered by open and closed savannah (Fig. 6). Overall, the configuration of soil erosion damages observed in the three different study plots is largely conform with the modelling result of soil erosion risk in the respective areas (Fig. 6).

As means of model validation systematic comparison of the RUSLE modelling result for soil erosion risk with the on-site field measurements of soil erosion damages, satisfactory performance of the modelling results can be pointed out (Fig. 6). Soil erosion risk modelling results for closed savannah test plot A1 and the corresponding on-site damages A2 show a strong spatial overlap and are significantly positively correlated ($R^2 = 0.69$, $n = 18$, $\alpha < 0.05$). This also applies for the mapping results for the open savannah ($R^2 = 0.71$, $n = 26$, $\alpha < 0.05$; Fig. 6b) and the settlement test plot ($R^2 = 0.58$, $n = 35$, $\alpha < 0.05$; Fig. 6c). On the whole, the model output of soil erosion risk for the entire 6 km^2 of plot areas and the on-site mapped 79 linear damage form shows a positive correlation with $R^2 = 0.61$ ($n = 79$). The analyses establish a statistical significance at $p < 0.05$ for the individual validations.

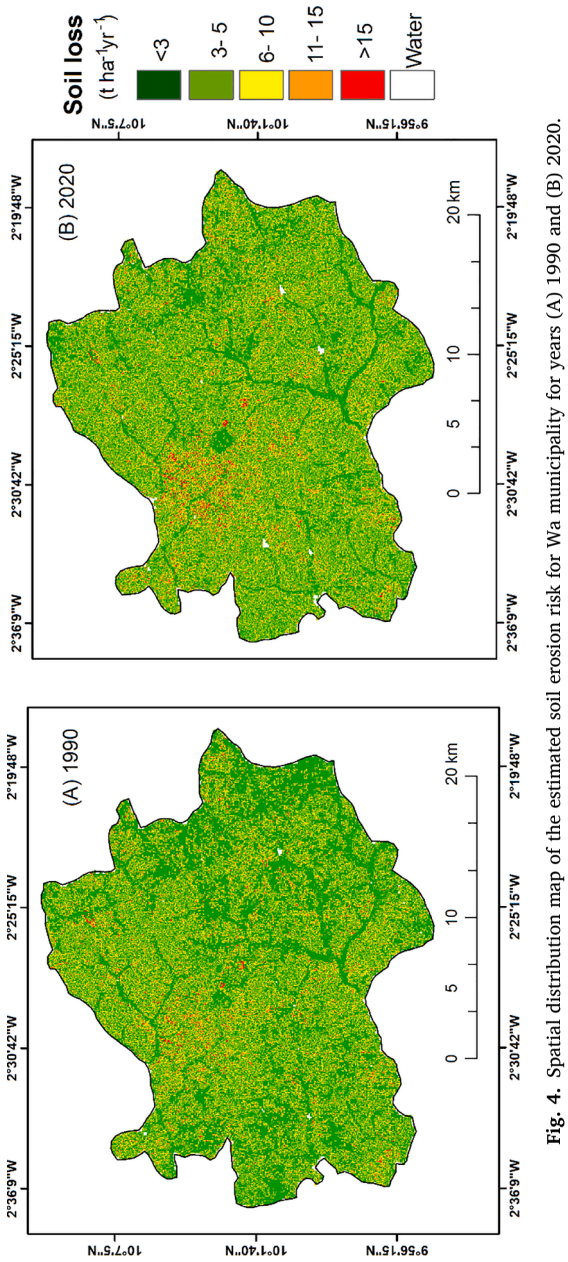

Fig. 4. Spatial distribution map of the estimated soil erosion risk for Wa municipality for years (A) 1990 and (B) 2020.

Table 4
Estimates of soil loss under different LULC across Wa municipality.

Land use	1990: Estimated soil loss by land use class				2020: Estimated soil loss by land use class			
	Total area (ha)	Total area (%)	Total soil loss (t y^{-1})	Total soil loss (%)	Total (ha)	Total area (%)	Total soil loss (t y^{-1})	Total soil loss (%)
Closed Savannah	12,869.0	22.2	14,584	9.7	9133.7	15.8	9627	4.8
Open Savannah	40,722.5	70.4	113,987	75.8	39,224.9	67.8	146,689	73.2
Other	22,18.1	3.8	18,549	12.3	2211.4	3.8	27,167	13.6
Settlement	744.4	1.3	1637	1.1	5985.9	10.4	13,794	6.9
Vegetated Wetland	1329.9	2.3	1644	1.1	1273.1	2.2	3187	1.6
	57,884.0	100	150,401	100	57,828.9	100.0	200,464	100

Discussion

The c. 30 % higher erosion risk predicted for the year 2020 than 1990 emphasize the RUSLE models results based on the prevailing driving factors in each year. These results are strongly linked to regional land use dynamics and changes in vegetation cover. The vegetation cover is essential in soil erosion risk reduction as its canopy intercepts rainfall, improves infiltration, and lowers the rainfall energy there by reducing its impacts on soil erosion [89]. The spatial distribution of soil erosion risks presented in the soil erosion risk map (Fig. 4) shows that areas with very high and extreme soil erosion risk correspond to areas with relatively low vegetation cover and slopes with steep gradients, a finding that corresponds to those among others of [81,90]. This especially applies to urbanized areas which occur in slopy terrain such as Bamahu, Kpelisisi Guli Kpelisi, Mungu, Duuli and the Wa township, which can be characterized as very high to severe rate of exposure to soil erosion risk. During the 30 years between 1990 and 2020 the areas with very high to severe exposure to soil erosion risk expanded, and this was triggered by urban spread and its associated alteration of vegetation cover. These findings correspond to those from other African strongly urbanizing areas such as Harare [86]. The observed significance of topographic characteristics (LS-factor) and cover factors as the main drivers for soil erosion risk within the Wa municipality is consistent with [89]. Beyond, [91] highlight the relevance of the slope length for controlling soil erosion risk.

The decrease in vegetation cover and the associated increase of soil erosion risk can be explained by the Wa municipality's increasing population and associated developmental activities [92]. Ghana's population and housing census has estimated a growth of the Wa municipality's population by 10 % between 2000 and 2010, counting 98,675 inhabitants in 2000 and 107,214 in 2010 [93]. A subsequent population and housing census conducted in 2021 attests a population growth to 200,672 inhabitants in Wa municipality [41], indicating a 6.0 % annual population growth since 2010. Population growth and associated settlement expansion drive infrastructure development, alteration of vegetation cover and environmental degradation as a whole [94,95]. Between 1990 and 2020 settlement spaces expanded spatially from 7.44 km^2 to 59.86 7.44 km^2 [45]. In parallel, the estimated soil loss for Wa municipality amounted 1637 tons in 1990 and octuplicates until 2020 to 13,794 tons in settlement areas. The settlement expansion-based soil erosion risk can be especially attributed to the infrastructure developments that need to be synchronized with the demands of population growth [94,96]. As the expansion of settlement areas is pronounced within the central part of Wa municipality where most settlements are clustered, construction of roads and other infrastructure developments are in progress. This leads to the destruction of the ecosystem and exposes surface material due to earth movements. In consequence, urbanization processes in Wa municipality led to the shrinking of areas covered by woody vegetation, a process especially due to the exploration of savannah vegetated areas for agriculture and other livelihood diversification options such as unregulated small-scale gold mining [73,97]. In total, an increase of settlement areas by 87.57 % between 1990 and 2020 in the Wa municipality parallel to a 40.89 % decrease of areas covered by woody vegetation [45] occurred. These changes in vegetation and land use are reflected in an estimated 25 % rise in total rate of soil loss between 1990 and 2020.

The strong control of soil erosion risk by LULC is also observed in areas under different savannah vegetation cover. In the year 1990 and 2020 area under open savannah vegetation in particulater contibuted to significant amount of soil loss due to proliferations of human activities within these areas, especially cultivation and grazing. Vulnerability to soil erosion corresponds to high soil erosion risk within the open savannah area with an escalating soil loss wherever canopy cover diminishes, ranging 2–4 t $ha^{-1}yr^{-1}$ in areas covered by trees and bushes and 16–34 t $ha^{-1}yr^{-1}$ for farmlands [98]. These data affirm the consequential effects of exploiting vegetated savannah areas within the Wa municipality for agriculture, which renders this area to high soil erosion risk.

Within the Wa municipality, seasonal bushfires (Plate 1), which generally occur during the Harmattan season [99], could be an exacerbating factor to increase soil erosion risk. Several studies pronounce the significant influence of bush fires on the rate of soil erosion [100,101]. According to Ref. [100], the severity level of bushfires is proportional to the rate of soil erosion. The interception functions of the trees canopy are lost after bushfire, thus, increased generation of surface run-off results and associated with soil detachment and sediment transport [102]. Estimated pre-fire soil erosion rates of 69 t $ha^{-1}yr^{-1}$ are distinctly lower than the estimated post-fire soil erosion rates (94 t $ha^{-1}yr^{-1}$) documenting that the soil erosion rate shortly after the fire event increased by 36.2 % [103]. However, it has to be considered that bush fires not only affect canopy cover but also soil characters as it is well known that a rise in soil water repellency is a frequent after-effect of bush and forest fires [104]. However, the long-term impact of fire on soil erosion could be higher than the immediate impact: An assessment of soil erosion after a decade of fire events shows a by a third reduced impact of fire on soil erosion compared to the impact observed immediately after bush fire event [103].

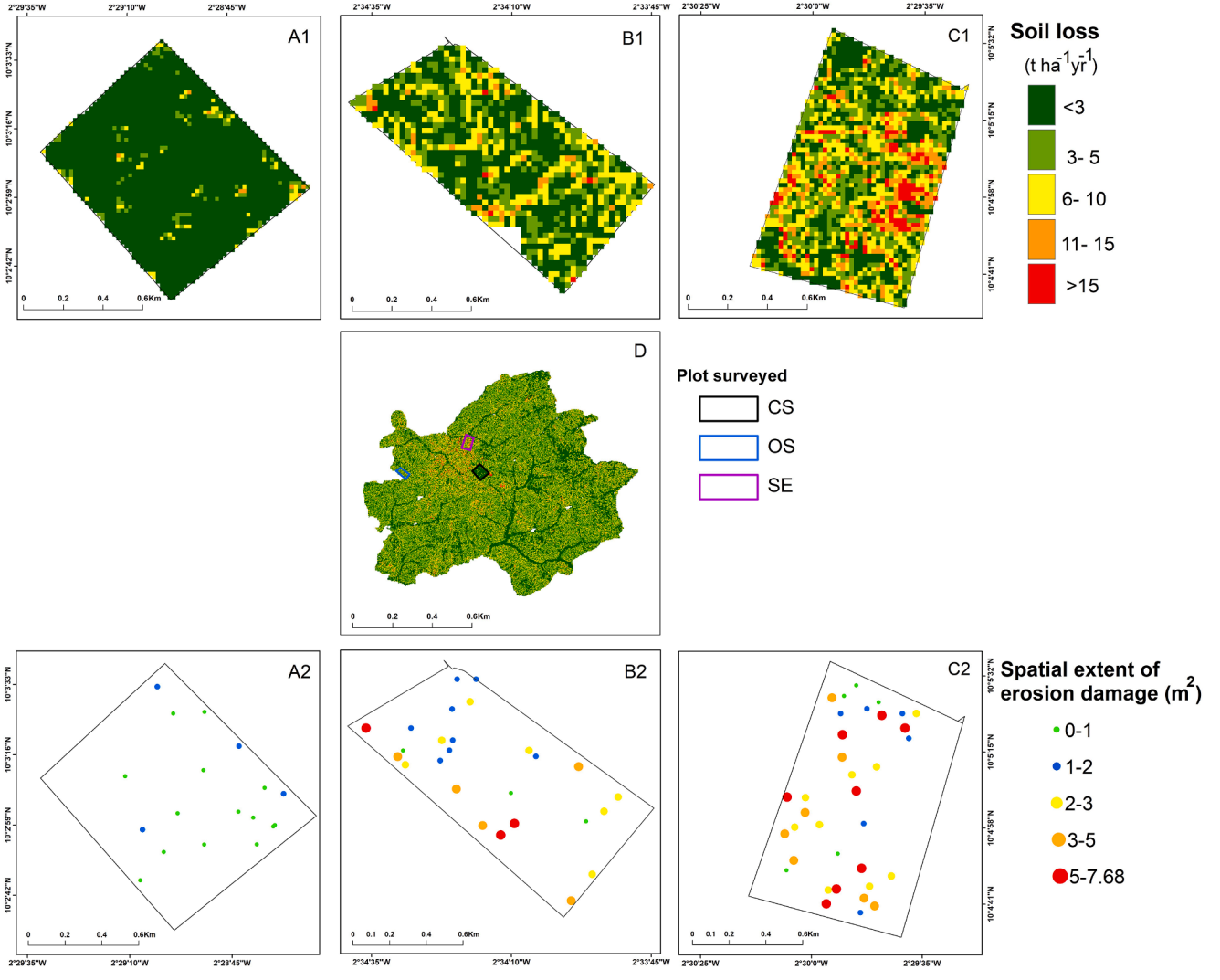

Fig. 5. Validation maps for model result and corresponding maps of field plots surveyed from January to February 2022. (A1) The 2 km^2 model output for closed savannah area with various levels of soil erosion risks for the year 2020; (B1) the 2 km^2 model output for open savannah area with various levels of soil erosion risks for the year 2020; (C1) the 2 km^2 model output for settlement area with various levels of soil erosion risks for the year 2020. (A2) the corresponding plot of A1 with 18 measured spatial extents of soil erosion damages; (B2) the corresponding plot of B1 with 26 measured spatial extents of soil erosion damages;(C2) the corresponding plot of C1 with 35 measured spatial extents of soil erosion damages. (D) The soil erosion risk map for the Wa municipality for the year 2020 from which A1, B1 and C1 were extracted.

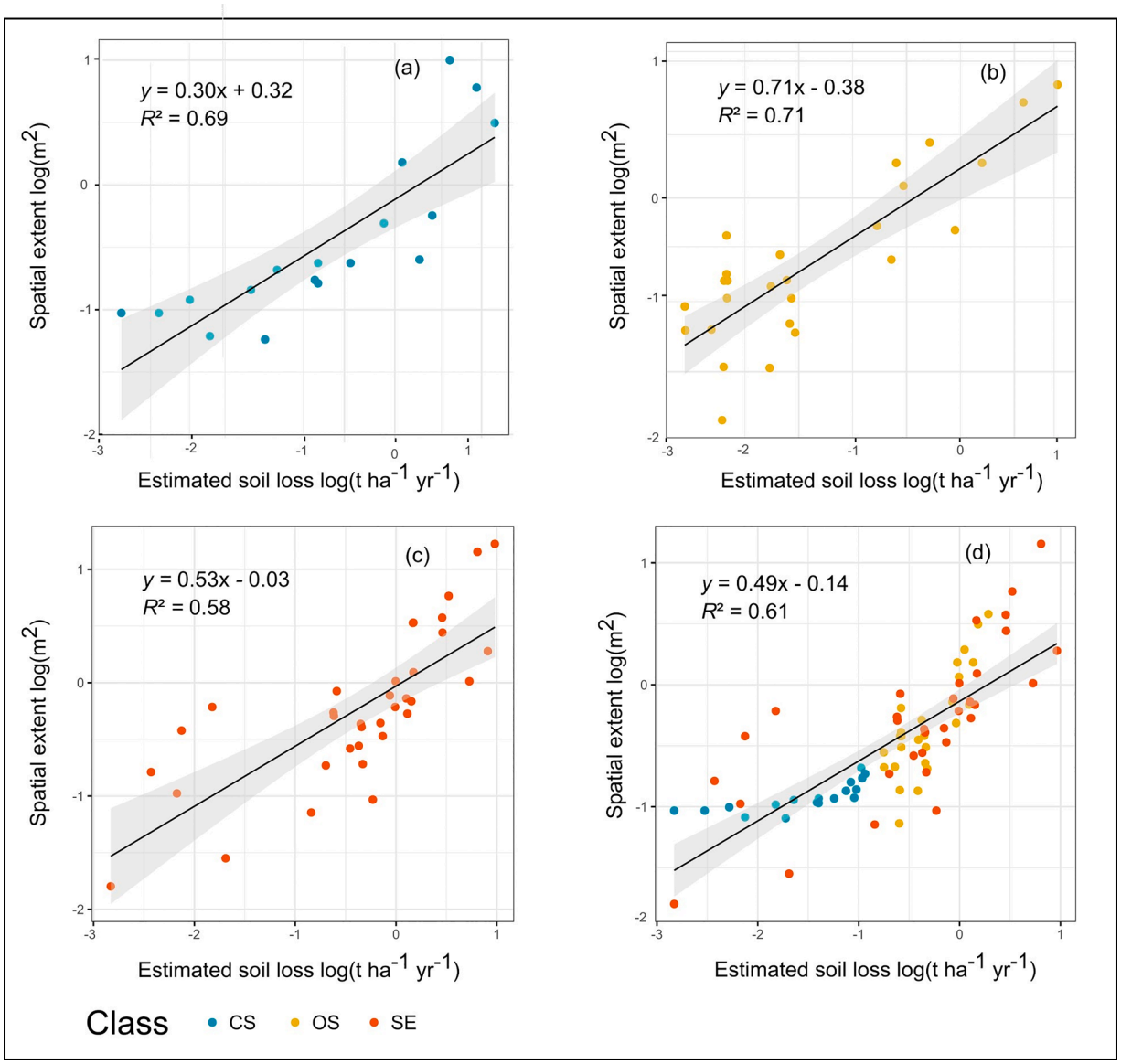

Fig. 6. Evaluation of the model's results and field measurement. (a) evaluation for closed savannah LULC class; (b) evaluation for open savannah LULC class (c) evaluation for settlement LULC class; (d) the combined evaluation of a, b and c.

The Wa municipality soils' physical characteristics and resulting erodibility potentials cause their low propensity to resist erosion [48].The dominance of sandy soil texture across Wa municipality and herein formed shallow savannah *ochrosols* and *laterites* is reflected in the distribution of soil erosion risk [42]. Coarse-textured soils dominate within the south-western part of the study municipality, resulting in moderate to severe soil erosion risks. Coarse-textured soils are in general characterized by high infiltration rates and corresponding low surface run-off generation; however, due to poor cohesion effects of sandy material erodibility is high [105, 106]. Also, the settlement areas of Nakore and Chansa township and the adjourning central part of the Wa municipality are characterized by widely spread soils with sandy texture and was estimated to have high-to-severe soil erosion risk. In contrast, soils with high clay content are characterized by relatively poor infiltration rates and consequently affect strong surface run-off generation, but due to the strong cohesion of clayey soils resistance capabilities are high and erodibility is low [107]. Beyond, soils with high aggregate stability resist the impact of raindrops and have a propensity to affect erosion [105,108]. In the North-western part of Wa municipality, soils with clayey texture are widely spread and frequently covered by savannah vegetation. These areas show low to moderate exposure to soil erosion risk owing to the combine detachment resistance properties of soil characters and soil coverage [41].

The RUSLE model's prediction of higher risk of potential erosion, compared to the actual risk of soil erosion is attributed to lack of vegetation cover and underlines the influence of the municipal's climate, soil and topographic characteristics on erosion. The climatic influence on potential erosion risk for the 1990 and 2020 is reflected in the R-factor maps (Fig. 2 C1 a and C2) and the corresponding

Plate 1. Soil erosion damages in the Wa municipality observed during the field survey. (CS) Damage observed within the closed savannah vegetation area; (OP) damages observed within the open savannah vegetation area; (SE) damage observed within the settlement area.

potential erosion risk maps (Fig. SM1 A and B). Thus, the spatial distribution of potential erosion risk is higher in the year 1990 than 2020 oweing to the higher amount and distribution of rainfall in the year 1990 than 2020. Increasing rainfall intensity and amount potentially increases soil detachment and soil erosion [109]. Beside the climatic influence on the potential erosion risk, the topographic characteristics of the study area control erosion as areas with steep slopes show the highest severity of potential erosoin risk [90].

The actual soil erosion risk map (Fig. 4) shows low soil erosion risk in areas with significant vegetation cover, while the corresponding areas on the potential risk of erosion map (Fig. SM1) shows "high" to "severe" risk. Most of the high to severe soil erosion risks were estimated for settlement and bareland areas while savannah vegetated areas underlie relatively low to moderate soil erosion risk. According to Ref. [110], human-induced modification of vegetation cover causes a high exposure to erosion risk in tropical landscapes. Unfortunately, the cover factor's function of erosion control is lacking in the settlement and bareland areas, consequently resulting in severe soil erosion risk [86] – and showing comparable exposure as the potential erosion risk.

The RUSLE model's predictions of soil erosion risk operate on the assumption of detachment of soil on the field [111]. The assessment of the model outputs is improved when data from field surveys (point-like plot-based data) are used for the validation [111, 112]. The data on spatial damages, estimated from the test-plots under different land use represent the effective amount of soil removed. These mapped damages correspond spatially with soil loss estimates generated using the RUSLE model. Settlement areas showed the highest spatial extent of effective soil erosion damage while closed and open savannah areas featured less spatial extent of eroded areas. The spatial extent of eroded areas in each of the test-plots agreed widely with the estimated soil erosion risk area applying the RUSLE model. Thus, the validation of the predicted soil erosion risk as provided by applying the RUSLE model by alignment with spatial extent of measured effective damages has been proven to be a suitable tool to affirm the reliability of a model application to a new environment. Statistical analyses established positive correlations between data resulting from the utilisation of the RUSLE model and on-site measured data. Overall, the statistics for the 79 point-based data from the field survey and the corresponding modelling are positively correlated and highly significant ($\alpha < 0.05$). Though field damage estimation could not account for damages based on sheet erosion, the spatial extent of damages from field measurements reflected the predicted output and enhanced model evaluation and validation. Despite the essence of long-term field measurement as an ideal means for empirical models validation in soil erosion estimation, plot-based point data are suitable for effective validation and the general comprehension of the model performance [111,113].

Conclusions

In the Savanna agro-ecological zones of Ghana soil erosion threatens environmental sustainability and agricultural productivity. Although predicting soil erosion risk is critical for developing land management plans sustainably in a vulnerable landscape, research in the Savannah agro-ecological zones has paid little consideration. This study assesses soil erosion risks within the context of land use dynamics in Wa municipality since 1990, a fast-developing area with rapid population growth. Assessment of soil erosion risk and estimation of average soil erosion rates per annum are based on a change detection of LULC in Wa municipality between 1990 and 2020 [45]. The application of the RUSLE model emphasizes in particular settlement areas and bareland in slopy terrain as highly vulnerable to soil erosion. The predicted rates of potential erosion for the years 1990 and 2020 were distinctly higher than the actual predicted rates of soil erosion of the respective years. The comparative lower actual soil erosion risk rate is due to vegetation cover influence that is reflected in the actual erosion risk model prediction for vegetated areas. Given the high risk associated with altered vegetated areas caused by human disturbances, the importance of a cover factor in soil conservation is emphasised. Aside the alteration of vegetation covers due to settlement activities, it is highlighting that areas with a high soil erosion risk spatially predominantly occur in areas with steep and long slopes.

Urbanization processes and settlement activities that cause changes and loss of vegetation cover can be attributed to the estimated c. 30 % increase of soil loss between 1990 and 2020. Though the modelling data as well as the field survey identify the settlement areas as a high-risk zone, it can also be pointed out that the open savannah area contributes distinctly to the total rate of soil loss. In consequence, since open savannah is the most widespread land cover class its contribution to total rate of soil loss is significant. In general, in Wa municipality the vegetation cover is largely altered through the exploration of the area for agriculture. These coupled with bushfire renders the area to high erosion risk. Due to the increasing population in Wa municipality, infrastructural development and agricultural production must synchronize with the populace's demands. Unfortunately, in the quest to achieve that, the conversion of vegetated areas into settlement areas and agricultural areas has led to significant soil erosion and in consequence land degradation in the Wa municipality. Especially settlement areas and bareland have been identified as areas being highly exposed to soil erosion risk. Overall, the soil erosion risk within the Wa municipality is strongly link to human-induced activities through land use intensification that renders the municipality vulnerable to erosion. Soil and water conservation strategies important in such situation, however, the field survey established that Wa municipality has no such interventions. It is therefore recommended to establish an integrated landscape management inclusive of soil and water conservation strategies to curtail the impending erosion-related menace. Findings from this study are relevant for designing and implementing mitigation strategies for the Wa municipality and tropical savannah landscapes at large. Outcomes of modelling soil erosion risk by applying the RUSLE in Wa municipality for the year 2020 was validated on a plot-based field survey conducted in January 2021. Statistical evaluations document an acceptable performance of the model output data. The statistics from the corroborative validation increase confidence in using the model.

Funding

We are thankful to German Academic Exchange Service (DAAD) for the award of fellowship through which this study was conducted. Also, we acknowledge and appreciate the Freie Universität Berlin who provided funds to publish this article.

CRediT authorship contribution statement

Mawuli Asempah: Conceptualization, Methodology, Validation, Formal analysis, Data curation, Writing – original draft. **Christopher Allan Shisanya:** Writing – review & editing, Supervision. **Brigitta Schütt:** Writing – review & editing, Supervision.

Declaration of Competing Interest

The authors declare that they have no known competing financial interests or personal relationships that could have appeared to influence the work reported in this paper.

Acknowledgements

We wish to express our profound gratitude to the colleagues at the Department of Earth Sciences, Freie Universität, Berlin for their valuable expert contributions that greatly contributed to the successful completion of this study. We wish to further appreciate colleagues at Water Resources Commission of Ghana, especially those within the Wa municipality, for their support that made the field survey a success. Finally, we are thankful to NASA, as well as the USGS where relevant data; specifically, SRTM DEM and Landsat satellite imageries were acquired for the study.

Supplementary materials

Supplementary material associated with this article can be found, in the online version, at doi:10.1016/j.sciaf.2023.e02042.

References

[1] M.J. Butt, A. Waqas, R. Mahmood, The combined effect of vegetation and soil erosion in the water resource management, Water Resour. Manag. 24 (2010) 3701–3714, https://doi.org/10.1007/s11269-010-9627-7.
[2] B.M. Mutua, A. Klik, W. Loiskandl, Modelling soil erosion and sediment yield at a catchment scale: the case of Masinga catchment, Kenya, L. Degrad. Dev. 17 (2006) 557–570, https://doi.org/10.1002/ldr.753.
[3] B.M. Flores, A. Staal, C.C. Jakovac, M. Hirota, M. Holmgren, R.S. Oliveira, Soil erosion as a resilience drain in disturbed tropical forests, Plant Soil (2019) 11–25, https://doi.org/10.1007/s11104-019-04097-8.
[4] K.M. Wantzen, J.H. Mol, Soil erosion from agriculture and mining: a threat to tropical stream ecosystems, Agriculture 3 (2013) 660–683, https://doi.org/10.3390/agriculture3040660.
[5] A.F. Arneth, F. Denton Agus, A. Elbehri, K. Erb, B. Osman Elasha, M. Rahimi, M. Rounsevell, A. Spence, R. Valentini, Framing and Context. In: Climate Change and Land: an IPCC special report on climate change, desertification, land degradation, sustainable land management, food security, and greenhouse gas fluxes in terrestrial ecosystems [P.R. Shukla, J. Skea, E. Calvo Buendia, V. Masson-Delmotte, H.-O. Pörtner, D.C. Roberts, P. Zhai, R. Slade, S. Connors, R. van Diemen, M. Ferrat, E. Haughey, S. Luz, S. Neogi, M. Pathak, J. Petzold, J. Portugal Pereira, P. Vyas, E. Huntley, K. Kissick, M. Belkacemi, J. Malley, (eds.)]. In press (2019) 77–129.
[6] C.A. Guerra, I.M.D. Rosa, E. Valentini, F. Wolf, F. Filipponi, D.N. Karger, A. Nguyen Xuan, J. Mathieu, P. Lavelle, N. Eisenhauer, Global vulnerability of soil ecosystems to erosion, Landsc. Ecol. 35 (2020) 823–842, https://doi.org/10.1007/s10980-020-00984-z.
[7] N. Labrière, B. Locatelli, Y. Laumonier, V. Freycon, M. Bernoux, Soil erosion in the humid tropics: a systematic quantitative review, Agric. Ecosyst. Environ. 203 (2015) 127–139, https://doi.org/10.1016/j.agee.2015.01.027.
[8] K.M. Chomitz, E. Brenes, L. Constantino, Financing environmental services: the Costa Rican experience and its implications, Sci. Total Environ. 240 (1999) 157–169, https://doi.org/10.1016/S0048-9697(99)00310-1.
[9] B. Locatelli, P. Imbach, R. Vignola, M.J. Metzger, E.J.L. Hidalgo, Ecosystem services and hydroelectricity in Central America: modelling service flows with fuzzy logic and expert knowledge, Reg. Environ. Change 11 (2011) 393–404, https://doi.org/10.1007/s10113-010-0149-x.
[10] Millennium Ecosystem Assessment. Ecosystems and Human Well-being: Opportunities and Challenges for Business and Industry, World Resources Institute, Washington, DC, 2005, pp. 1–33.
[11] P. Borrelli, C. Alewell, P. Alvarez, J.A.A. Anache, J. Baartman, C. Ballabio, N. Bezak, M. Biddoccu, A. Cerdà, D. Chalise, S. Chen, W. Chen, A.M. De Girolamo, G. D. Gessesse, D. Deumlich, N. Diodato, N. Efthimiou, G. Erpul, P. Fiener, M. Freppaz, F. Gentile, A. Gericke, N. Haregeweyn, B. Hu, A. Jeanneau, K. Kaffas, M. Kiani-Harchegani, I.L. Villuendas, C. Li, L. Lombardo, M. López-Vicente, M.E. Lucas-Borja, M. Märker, F. Matthews, C. Miao, M. Mikoš, S. Modugno, M. Möller, V. Naipal, M. Nearing, S. Owusu, D. Panday, E. Patault, C.V. Patriche, L. Poggio, R. Portes, L. Quijano, M.R. Rahdari, M. Renima, G.F. Ricci, J. Rodrigo-Comino, S. Saia, A.N. Samani, C. Schillaci, V. Syrris, H.S. Kim, D.N. Spinola, P.T. Oliveira, H. Teng, R. Thapa, K. Vantas, D. Vieira, J.E. Yang, S. Yin, D.A. Zema, G. Zhao, P. Panagos, Soil erosion modelling: a global review and statistical analysis, Sci. Total Environ. 780 (2021), https://doi.org/10.1016/j.scitotenv.2021.146494.
[12] P. Borrelli, D.A. Robinson, L.R. Fleischer, E. Lugato, C. Ballabio, C. Alewell, K. Meusburger, S. Modugno, B. Schütt, V. Ferro, V. Bagarello, K. Van Oost, L. Montanarella, P. Panagos, An assessment of the global impact of 21st century land use change on soil erosion, Nat. Commun. 8 (2017), https://doi.org/10.1038/s41467-017-02142-7.
[13] Intergovernmental Panel on Climate Change (IPCC), Summary for Policymakers. In: Climate Change and Land: an IPCC special report on climate change, desertification, land degradation, sustainable land management, food security, and greenhouse gas fluxes in terrestrial ecosystems [P.R. Shukla, J. Skea, E. Calvo Buendia, V. Masson-Delmotte, H.- O. Pörtner, D. C. Roberts, P. Zhai, R. Slade, S. Connors, R. van Diemen, M. Ferrat, E. Haughey, S. Luz, S. Neogi, M. Pathak, J. Petzold, J. Portugal Pereira, P. Vyas, E. Huntley, K. Kissick, M. Belkacemi, J. Malley, (eds.)], In press, 2019, ISBN 978-92-9169-154-8.
[14] R. Lal, Soil erosion and the global carbon budget, Environ. Int. 29 (2003) 437–450, https://doi.org/10.1016/S0160-4120(02)00192-7.

[15] D. Pimentel, C. Harvey, P. Resosudarmo, K. Sinclair, D. Kurz, M. McNair, S. Crist, L. Shpritz, L. Fitton, R. Saffouri, R. Blair, Environmental and economic costs of soil erosion and conservation benefits, Science (80-.) 267 (1995) 1117–1123, https://doi.org/10.1126/science.267.5201.1117.

[16] H.E. Dregne, Land degradation in the drylands, Arid. Land Res. Manag. 16 (2002) 99–132, https://doi.org/10.1080/153249802317304422.

[17] S.E. Obalum, M.M. Buri, J.C. Nwite, Hermansah, Y. Watanabe, C.A. Igwe, T. Wakatsuki, Soil degradation-induced decline in productivity of sub-saharan african soils: the prospects of looking downwards the lowlands with the sawah ecotechnology, Appl. Environ. Soil Sci. 2012 (2012), https://doi.org/10.1155/2012/673926.

[18] A.A. Fenta, A. Tsunekawa, N. Haregeweyn, J. Poesen, M. Tsubo, P. Borrelli, P. Panagos, M. Vanmaercke, J. Broeckx, H. Yasuda, T. Kawai, Y. Kurosaki, Land susceptibility to water and wind erosion risks in the East Africa region, Sci. Total Environ. 703 (2020), https://doi.org/10.1016/j.scitotenv.2019.135016.

[19] F.A.Y. Okou, B. Tente, Y. Bachmann, B. Sinsin, Regional erosion risk mapping for decision support: a case study from West Africa, Land Use Policy 56 (2016) 27–37, https://doi.org/10.1016/j.landusepol.2016.04.036.

[20] B.N. Baatuuwie, K. Ochire-Boadu, S. Abdul-Ganiyu, W.J. Asante, Assessment of soil and water conservation measures practiced by farmers: a case study in the Tolon-Kumbungu District of Northern Ghana, J. Soil Sci. Environ. Manag. 2 (2011) 103–109.

[21] A.W. Moomen, A. Dewan, Assessing the spatial relationships between mining and land degradation: evidence from Ghana, Int. J. Mining, Reclam. Environ. 31 (2017) 505–518, https://doi.org/10.1080/17480930.2016.1188253.

[22] C. Yin, W. Zhao, P. Pereira, Soil conservation service underpins sustainable development goals, Glob. Ecol. Conserv. 33 (2022) e01974, https://doi.org/10.1016/j.gecco.2021.e01974.

[23] A. Foucher, S. Salvador-Blanes, O. Evrard, A. Simonneau, E. Chapron, T. Courp, O. Cerdan, I. Lefèvre, H. Adriaensen, F. Lecompte, M. Desmet, Increase in soil erosion after agricultural intensification: evidence from a lowland basin in France, Anthropocene 7 (2014) 30–41, https://doi.org/10.1016/j.ancene.2015.02.001.

[24] L. Eisazadeh, R. Sokouti, M. Homaee, E. Pazira, Comparison of empirical models to estimate soil erosion and sediment yield in micro catchments, Eurasian J. Soil Sci. 1 (2012) 28–33.

[25] P.U. Igwe, A.A. Onuigbo, O.C. Chinedu, I.I. Ezeaku, M.M. Muoneke, Soil erosion: a review of models and applications, Int. J. Adv. Eng. Res. Sci. 4 (2017) 138–150, https://doi.org/10.22161/ijaers.4.12.22.

[26] M. Abdullah, R. Feagin, L. Musawi, The use of spatial empirical models to estimate soil erosion in arid ecosystems, Environ. Monit. Assess. 189 (2017), https://doi.org/10.1007/s10661-017-5784-y.

[27] K. Meusburger, N. Konz, M. Schaub, C. Alewell, Soil erosion modelled with USLE and PESERA using QuickBird derived vegetation parameters in an alpine catchment, Int. J. Appl. Earth Obs. Geoinf. 12 (2010) 208–215, https://doi.org/10.1016/j.jag.2010.02.004.

[28] W.S. Merritt, R.A. Letcher, A.J. Jakeman, A review of erosion and sediment transport models, Environ. Model. Softw. 18 (2003) 761–799, https://doi.org/10.1016/S1364-8152(03)00078-1.

[29] R. Ranzi, T.H. Le, M.C. Rulli, A RUSLE approach to model suspended sediment load in the Lo river (Vietnam): effects of reservoirs and land use changes, J. Hydrol. 422-423 (2012) 17–29, https://doi.org/10.1016/j.jhydrol.2011.12.009.

[30] W.H. Wischmeier, D.D. Smith, Predicting Rainfall Erosion Losses: A Guide to Conservation Planning, Department of Agriculture, Science and Education Administration, 1978.

[31] K. Renard, G. Foster, G. Weesies, D. McCool, D. Yoder, Predicting Soil Erosion By Water: A Guide to Conservation Planning With the Revised Universal Soil Loss Equation (RUSLE), United States Government Printing, 1997. http://www.ars.usda.gov/SP2UserFiles/Place/64080530/RUSLE/AH_703.pdf.

[32] J.G. Arnold, R. Srinivasan, R.S. Muttiah, J.R. Williams, basin scale model called SWAT (Soil and Water speed and storage, advanced software debugging policy to meet the needs, and the management to the tank model, J. Am. Water Resour. Assoc. 34 (1998) 73–89.

[33] J.M. Laflen, W.J. Elliot, J.R. Simanton, C.S. Holzhey, K.D. Kohl, WEPP: soil erodibility experiments for rangeland and cropland soils, J. Soil Water Conserv. 46 (1991) 39–44.

[34] D. Chalise, L. Kumar, C.P. Shriwastav, S. Lamichhane, Spatial assessment of soil erosion in a hilly watershed of Western Nepal, Environ. Earth Sci. 77 (2018), https://doi.org/10.1007/s12665-018-7842-3, 0.

[35] A. Shamshad, M.N. Azhari, M.H. Isa, W.M.A.W. Hussin, B.P. Parida, Development of an appropriate procedure for estimation of RUSLE EI30 index and preparation of erosivity maps for Pulau Penang in Peninsular Malaysia, Catena 72 (2008) 423–432, https://doi.org/10.1016/j.catena.2007.08.002.

[36] G. Wang, G. Gertner, S. Fang, A.B. Anderson, Mapping multiple variables for predicting soil loss by geostatistical methods with TM images and a slope map, Photogramm. Eng. Remote Sens. 69 (2003) 889–898, https://doi.org/10.14358/PERS.69.8.889.

[37] R. Benavidez, J. Bethanna, M. Deborah, N. Kevin, A-review-of-the-revised-universal-soil-loss-equation-RUSLE-with-a-view-to-increasing-its-global-applicability-and-improving-soil-loss-estimates2018 Hydrology-and-Earth-System-SciencesOpen-Access.pdf Hydrol, Earth Syst. Sci. 22 (2018) 6059–6086, https://doi.org/10.5194/hess-22-6059-2018.

[38] C. Schürz, B. Mehdi, J. Kiesel, K. Schulz, M. Herrnegger, A systematic assessment of uncertainties in large-scale soil loss estimation from different representations of USLE input factors-a case study for Kenya and Uganda, Hydrol. Earth Syst. Sci. 24 (2020) 4463–4489, https://doi.org/10.5194/hess-24-4463-2020.

[39] M. Constantine, K.N. Ogbu, Assessment of soil erosion using RUSLE2 model and GIS in Upper Ebonyi River Watershed, Enugu State, Nigeria, Int. J. Remote Sens. Geosci. 4 (2015) 7–17.

[40] Ghana Statistical Service, Policy Implications of Population Trends, Population Data Analysis Reports 2, Ghana Statistical Service, Accra, Ghana, 2005, pp. 1–495.

[41] Ghana Statistical Service, Ghana 2021 population and housing cencus: population of regions and districts, 3A (2021) 1–6.

[42] Ghana Statistics Service, The 2010 Population and Housing Census: District Analytical Report, Wa Municipality, in: K. Awusabo-Asare, N.N.N. Nsowah-Nuamah, A.K. Anaman, S.K. Gaisie (Eds.), Ghana Statistics Service, Accra, Ghana, 2014, pp. 1–67.

[43] B. Barry, E. Obuobie, M. Andreini, W. Andah, M. Pluquet, Comprehensive Assessment of Water Management in Agriculture. Comparative Study of River Basin Development and Management, International Water Management Institute IWMI (2005) 1–187.

[44] D. Kpienbaareh, J.O. Appiah, A geospatial approach to assessing land change in the built-up landscape of Wa Municipality of Ghana, Geogr. Tidsskr. - Danish J. Geogr. 119 (2019) 121–135, https://doi.org/10.1080/00167223.2019.1587307.

[45] M. Asempah, W. Sahwan, B. Schütt, Assessment of land cover dynamics and drivers of urban expansion using geospatial and logistic regression approach in wa municipality, ghana, Land 10 (2021), https://doi.org/10.3390/land10111251 (Basel).

[46] J.R. Ham, Cooking to be modern but eating to be healthy: the role of Dawa-Dawa in contemporary ghanaian foodways, Food Cult. Soc. 20 (2017) 237–256, https://doi.org/10.1080/15528014.2017.1305827.

[47] R. Kent, “Helping” or “appropriating”? Gender relations in shea nut production in Northern Ghana, Soc. Nat. Resour. 31 (2018) 367–381, https://doi.org/10.1080/08941920.2017.1382626.

[48] S. Beguería, M. Angulo-Martínez, L. Gaspar, A. Navas, Detachment of soil organic carbon by rainfall splash: experimental assessment on three agricultural soils of Spain, Geoderma 245–246 (2015) 21–30, https://doi.org/10.1016/j.geoderma.2015.01.010.

[49] T. Hengl, J.M. De Jesus, G.B.M. Heuvelink, M.R. Gonzalez, M. Kilibarda, A. Blagotić, W. Shangguan, M.N. Wright, X. Geng, B. Bauer-Marschallinger, M.A. Guevara, R. Vargas, R.A. MacMillan, N.H. Batjes, J.G.B. Leenaars, E. Ribeiro, I. Wheeler, S. Mantel, B. Kempen, SoilGrids250m: global gridded soil information based on machine learning, 2017. doi:https://doi.org/10.1371/journal.pone.0169748.

[50] Y. Yang, R. Zhao, Z. Shi, R.A. Viscarra Rossel, D. Wan, Z. Liang, Integrating multi-source data to improve water erosion mapping in Tibet, China, Catena 169 (2018) 31–45, https://doi.org/10.1016/j.catena.2018.05.021.

[51] A.N. Sharpley, J.R. Williams, EPIC: The erosion-Productivity Impact Calculator, U.S. Dep. Agric. Tech. Bull., 1990, p. 235. http://agris.fao.org/agris-search/search.do?recordID=US9403696.

[52] S. Schmidt, S. Tresch, K. Meusburger, Modification of the RUSLE slope length and steepness factor (LS-factor) based on rainfall experiments at steep alpine grasslands, MethodsX 6 (2019) 219–229, https://doi.org/10.1016/j.mex.2019.01.004.

[53] Y. Farhan, S. Nawaiseh, Spatial assessment of soil erosion risk using RUSLE and GIS techniques, Environ. Earth Sci. 74 (2015) 4649–4669, https://doi.org/10.1007/s12665-015-4430-7.
[54] M.B. Defersha, S. Quraishi, A. Melesse, Interrill erosion, runoff and sediment size distribution as affected by slope steepness and antecedent moisture content, Hydrol. Earth Syst. Sci. Discuss. 7 (2010) 6447–6489, https://doi.org/10.5194/hessd-7-6447-2010.
[55] D.M. Fox, R.B. Bryan, The relationship of soil loss by interrill erosion to slope gradient, Catena 38 (2000) 211–222, https://doi.org/10.1016/S0341-8162(99)00072-7.
[56] D.P. Shrestha, V.G. Jetten, Modelling erosion on a daily basis, an adaptation of the MMF approach, Int. J. Appl. Earth Obs. Geoinf. 64 (2018) 117–131, https://doi.org/10.1016/j.jag.2017.09.003.
[57] L. Wang, H. Liu, An efficient method for identifying and filling surface depressions in digital elevation models for hydrologic analysis and modelling, Int. J. Geogr. Inf. Sci. 20 (2006) 193–213, https://doi.org/10.1080/13658810500433453.
[58] S. Wu, J. Li, G.H. Huang, A study on DEM-derived primary topographic attributes for hydrologic applications: sensitivity to elevation data resolution, Appl. Geogr. 28 (2008) 210–223, https://doi.org/10.1016/j.apgeog.2008.02.006.
[59] D.G. Tarboton, A new method for the determination of flow directions and upslope areas in grid digital elevation models, Water Resour. Res. 33 (1997) 309–319.
[60] X. Yang, Digital mapping of RUSLE slope length and steepness factor across New South Wales, Australia, Soil Res. 53 (2015) 216–225, https://doi.org/10.1071/SR14208.
[61] M.A. Stocking, H.A. Elwell, Rainfall erosivity over Rhodesia, Trans. Inst. Br. Geogr. 1 (1976) 231–245, https://doi.org/10.2307/621986.
[62] D.T. Meshesha, A. Tsunekawa, M. Tsubo, N. Haregeweyn, E. Adgo, Distribution de la taille de gouttes de pluie et de l'énergie cinétique des précipitations dans les hautes terres de la vallée du Rift Central, Ethiopie, Hydrol. Sci. J. 59 (2014) 2203–2215, https://doi.org/10.1080/02626667.2013.865030.
[63] J. Thomas, S. Joseph, K.P. Thrivikramji, Assessment of soil erosion in a tropical mountain river basin of the southern Western Ghats, India using RUSLE and GIS, Geosci. Front. 9 (2018) 893–906, https://doi.org/10.1016/j.gsf.2017.05.011.
[64] J.H. Lee, J.H. Heo, Evaluation of estimation methods for rainfall erosivity based on annual precipitation in Korea, J. Hydrol. 409 (2011) 30–48, https://doi.org/10.1016/j.jhydrol.2011.07.031.
[65] K.G. Renard, J.R. Freimund, Using monthly precipitation data to estimate the R-factor in the revised USLE, J. Hydrol. 157 (1994) 287–306, https://doi.org/10.1016/0022-1694(94)90110-4.
[66] H. Tilahun, G. Taddesse, A. Melese, T. Mebrate, Assessment of spatial soil erosion hazard in Ajema Watershed, North Shewa Zone, Ethiopia, Adv. Plants Agric. Res. Res. 8 (2018) 552–558, https://doi.org/10.15406/apar.2018.08.00384.
[67] S. Lee, Soil erosion assessment and its verification using the universal soil loss equation and geographic information system: a case study at Boun, Korea, Environ. Geol. 45 (2004) 457–465, https://doi.org/10.1007/s00254-003-0897-8.
[68] D. Mengistu, W. Bewket, R. Lal, Sustainable intensification to advance food security and enhance climate resilience in Africa, Sustain, Intensif. to Adv. Food Secur. Enhanc. Clim. Resil. Africa. (2015) 137–163, https://doi.org/10.1007/978-3-319-09360-4.
[69] M. Wynants, H. Solomon, P. Ndakidemi, W.H. Blake, Pinpointing areas of increased soil erosion risk following land cover change in the Lake Manyara catchment, Tanzania, Int. J. Appl. Earth Obs. Geoinf. 71 (2018) 1–8.
[70] L. Benkobi, M.J. Trlica, J.L. Smith, Evaluation of a refined surface cover subfactor for use in RUSLE, J. Range Manag. 47 (1994) 74–78, https://doi.org/10.2307/4002845.
[71] J. Wu, Y. Kurosaki, B. Gantsetseg, M. Ishizuka, T.T. Sekiyama, B. Buyantogtokh, J. Liu, Estimation of dry vegetation cover and mass from MODIS data: verification by roughness length and sand saltation threshold, Int. J. Appl. Earth Obs. Geoinf. 102 (2021), 102417, https://doi.org/10.1016/j.jag.2021.102417.
[72] H. Tanyaş, Ç. Kolat, M.L. Süzen, A new approach to estimate cover-management factor of RUSLE and validation of RUSLE model in the watershed of Kartalkaya Dam, J. Hydrol. 528 (2015) 584–598, https://doi.org/10.1016/j.jhydrol.2015.06.048.
[73] P.L. Basommi, Q. Guan, D. Cheng, Exploring Land use and Land cover change in the mining areas of Wa East District, Ghana using satellite imagery, Open Geosci. 7 (2015) 618–626, https://doi.org/10.1515/geo-2015-0058.
[74] J.M. Kusimi, E.M. Attua, Soil erosion and sediment yield modelling in the Pra River Basin of Ghana using the revised universal soil loss equation (RUSLE), Ghana J. Geogr. 7 (2015) 38–57.
[75] G. Watene, L. Yu, Y. Nie, J. Zhu, T. Ngigi, J.D.D. Nambajimana, B. Kenduiywo, Water erosion risk assessment in the Kenya great rift valley region, Sustainability 13 (2021) 1–31, https://doi.org/10.3390/su13020844.
[76] J. Kusimi, G.A.B.Y. Manyimadin, E.M. Attua, Soil erosion and sediment yield modelling in the Pra River Basin of Ghana using the revised universal soil loss equation (RUSLE), Ghana J. Geogr. 7 (2015) 38–57.
[77] J.K. Asiedu, Assessing the threat of erosion to nature-based interventions for stormwater management and flood control in the Greater Accra Metropolitan Area, Ghana, J. Ecol. Eng. 19 (2018) 1–13, https://doi.org/10.12911/22998993/79418.
[78] R. Girma, E. Gebre, Spatial modeling of erosion hotspots using GIS-RUSLE interface in Omo-Gibe river basin, Southern Ethiopia: implication for soil and water conservation planning, Environ. Syst. Res. 9 (2020), https://doi.org/10.1186/s40068-020-00180-7.
[79] P. Karthick, C. Lakshumanan, P. Ramki, Estimation of soil erosion vulnerability in Perambalur Taluk, Tamilnadu using revised universal soil loss equation model (RUSLE) and geo information technology, Int. Res. J. Earth Sci. 5 (2017) 8–14.
[80] P. Panagos, P. Borrelli, K. Meusburger, E.H. van der Zanden, J. Poesen, C. Alewell, Modelling the effect of support practices (P-factor) on the reduction of soil erosion by water at European scale, Environ. Sci. Policy. 51 (2015) 23–34, https://doi.org/10.1016/j.envsci.2015.03.012.
[81] P. Tian, Z. Zhu, Q. Yue, Y. He, Z. Zhang, F. Hao, W. Guo, L. Chen, M. Liu, Soil erosion assessment by RUSLE with improved P factor and its validation: case study on mountainous and hilly areas of Hubei Province, China, Int. Soil Water Conserv. Res. 9 (2021) 433–444, https://doi.org/10.1016/j.iswcr.2021.04.007.
[82] P. Panagos, P. Borrelli, J. Poesen, C. Ballabio, E. Lugato, K. Meusburger, L. Montanarella, C. Alewell, The new assessment of soil loss by water erosion in Europe, Environ. Sci. Policy 54 (2015) 438–447, https://doi.org/10.1016/j.envsci.2015.08.012.
[83] J. Chen, H. Xiao, Z. Li, C. Liu, D. Wang, L. Wang, C. Tang, Threshold effects of vegetation coverage on soil erosion control in small watersheds of the red soil hilly region in China, Ecol. Eng. 132 (2019) 109–114, https://doi.org/10.1016/j.ecoleng.2019.04.010.
[84] W. Bewket, G. Sterk, Assessment of soil erosion in cultivated fields using a survey methodology for rills in the Chemoga watershed, Ethiopia, Agric. Ecosyst. Environ. 97 (2003) 81–93, https://doi.org/10.1016/S0167-8809(03)00127-0.
[85] J. Poesen, J. Nachtergaele, G. Verstraeten, C. Valentin, Gully erosion and environmental change: importance and research needs, Catena 50 (2003) 91–133, https://doi.org/10.1016/S0341-8162(02)00143-1.
[86] A.K. Marondedze, B. Schütt, Assessment of soil erosion using the rusle model for the Epworth district of the Harare metropolitan province, Zimbabwe, Sustainability 12 (2020) 1–24, https://doi.org/10.3390/su12208531.
[87] T. Melese, A. Senamaw, T. Belay, G. Bayable, The spatiotemporal dynamics of land use land cover change, and its impact on soil erosion in Tagaw Watershed, Blue Nile Basin, Ethiopia, Glob. Chall. 5 (2021), 2000109, https://doi.org/10.1002/gch2.202000109.
[88] M. Mariye, M. Mariyo, Y. Changming, Z.L. Teffera, B. Weldegebrial, Effects of land use and land cover change on soil erosion potential in Berhe district: a case study of Legedadi watershed, Ethiopia, Int. J. River Basin Manag. 20 (2022) 79–91, https://doi.org/10.1080/15715124.2020.1767636.
[89] K. Uddin, M.A. Matin, S. Maharjan, Assessment of land cover change and its impact on changes in soil erosion risk in Nepal, Sustainability 10 (2018), https://doi.org/10.3390/su10124715.
[90] D. Pimentel, M. Burgess, Soil erosion threatens food production, Agriculture 3 (2013) 443–463, https://doi.org/10.3390/agriculture3030443.
[91] F. Karamage, C. Zhang, X. Fang, T. Liu, F. Ndayisaba, L. Nahayo, A. Kayiranga, J.B. Nsengiyumva, Modeling rainfall-runoffresponse to land use and land cover change in Rwanda (1990-2016), Water 9 (2017), https://doi.org/10.3390/w9020147 (Switzerland).
[92] S.S. Myers, L. Gaffikin, C.D. Golden, R.S. Ostfeld, K.H. Redford, T.H. Ricketts, W.R. Turner, S.A. Osofsky, Human health impacts of ecosystem alteration, Proc. Natl. Acad. Sci. U. S. A. 110 (2013) 18753–18760, https://doi.org/10.1073/pnas.1218656110.

[93] GSS, 2010 Population and Housing Census, summary of Report of final results, 2012, pp. 1–117. Ghana Stat. Serv.
[94] R.A. Acheampong, P.A. Anokye, Understanding households' residential location choice in Kumasi's Peri-urban settlements and the implications for sustainable urban growth, Res. Humanit. Soc. Sci. 3 (2013) 60–70.
[95] D.O. Appiah, J.T. Bugri, E.K. Forkuo, P.K. Boateng, Determinants of peri-urbanization and land use change patterns in peri-urban Ghana, J. Sustain. Dev. 7 (2014) 95–109, https://doi.org/10.5539/jsd.v7n6p95.
[96] I.K. Osumanu, J.N. Akongbangre, G.N.Y. Tuu, E. Owusu-Sekyere, From patches of villages to a municipality: time, space, and expansion of Wa, Ghana, Urban Forum 30 (2019) 57–74, https://doi.org/10.1007/s12132-018-9341-8.
[97] R. Antabe, K.N. Atuoye, V.Z. Kuuire, Y. Sano, G. Arku, I. Luginaah, Community health impacts of surface mining in the Upper West Region of Ghana: the roles of mining odors and dust, Hum. Ecol. Risk Assess. 23 (2017) 798–813, https://doi.org/10.1080/10807039.2017.1285691.
[98] B. Diwediga, Q.B. Le, S.K. Agodzo, L.D. Tamene, K. Wala, Modelling soil erosion response to sustainable landscape management scenarios in the Mo River Basin (Togo, West Africa), Sci. Total Environ. 625 (2018) 1309–1320, https://doi.org/10.1016/j.scitotenv.2017.12.228.
[99] A.K. Yahaya, S.T. Amoah, Bushfires in the Nandom district of the Upper West Region of Ghana: perpetual threat to food crop production, J. Environ. Earth Sci. 3 (2013) 10–14. http://citeseerx.ist.psu.edu/viewdoc/download?doi=10.1.1.875.3490&rep=rep1&type=pdf.
[100] A.A. Agbeshie, S. Abugre, T. Atta-Darkwa, R. Awuah, A review of the effects of forest fire on soil properties, J. For. Res. (2022), https://doi.org/10.1007/s11676-022-01475-4.
[101] J.J. O'Brien, J.K. Hiers, J.M. Varner, C.M. Hoffman, M.B. Dickinson, S.T. Michaletz, E.L. Loudermilk, B.W. Butler, Advances in mechanistic approaches to quantifying biophysical fire effects, Curr. For. Rep. 4 (2018) 161–177, https://doi.org/10.1007/s40725-018-0082-7.
[102] A. Bento-Gonçalves, A. Vieira, Wildfires in the wildland-urban interface: key concepts and evaluation methodologies, Sci. Total Environ. 707 (2020), 135592, https://doi.org/10.1016/j.scitotenv.2019.135592.
[103] N. Depountis, M. Michalopoulou, K. Kavoura, K. Nikolakopoulos, N. Sabatakakis, Estimating soil erosion rate changes in areas affected by wildfires, ISPRS Int. J. Geo-Inf. 9 (2020), https://doi.org/10.3390/ijgi9100562.
[104] Y. Kusakari, K.O. Asubonteng, G.S. Jasaw, F. Dayour, T. Dzivenu, V. Lolig, S.A. Donkoh, F.K. Obeng, B. Gandaa, G. Kranjac-Berisavljevic, Farmer-perceived effects of climate change on livelihoods in WA west district, upper west region of Ghana, J. Disaster Res. 9 (2014) 516–528, https://doi.org/10.20965/jdr.2014.p0516.
[105] P.M. Fox, P.S. Nico, M.M. Tfaily, K. Heckman, J.A. Davis, Characterization of natural organic matter in low-carbon sediments: extraction and analytical approaches, Org. Geochem. 114 (2017) 12–22, https://doi.org/10.1016/j.orggeochem.2017.08.009.
[106] S.W. Duiker, D.C. Flanagan, R. Lal, Erodibility and infiltration characteristics of five major soils of southwest Spain, Catena 45 (2001) 103–121, https://doi.org/10.1016/S0341-8162(01)00145-X.
[107] K. Zhang, Y. Yu, J. Dong, Q. Yang, X. Xu, Agriculture, ecosystems and environment adapting & testing use of USLE K factor for agricultural soils in China, Agric. Ecosyst. Environ. 269 (2019) 148–155, https://doi.org/10.1016/j.agee.2018.09.033.
[108] O. Fox, S. Vetter, K. Ekschmitt, V. Wolters, Soil fauna modifies the recalcitrance-persistence relationship of soil carbon pools, Soil Biol. Biochem. 38 (2006) 1353–1363, https://doi.org/10.1016/j.soilbio.2005.10.014.
[109] M.A. Mohamadi, A. Kavian, Effects of rainfall patterns on runoff and soil erosion in field plots, Int. Soil Water Conserv. Res. 3 (2015) 273–281, https://doi.org/10.1016/j.iswcr.2015.10.001.
[110] S. Ullah, A. Ali, M. Iqbal, M. Javid, M. Imran, Geospatial assessment of soil erosion intensity and sediment yield: a case study of Potohar Region, Pakistan, Environ. Earth Sci. 77 (2018) 1–13, https://doi.org/10.1007/s12665-018-7867-7.
[111] K.E. Seutloali, T. Dube, O. Mutanga, Assessing and mapping the severity of soil erosion using the 30-m Landsat multispectral satellite data in the former South African homelands of Transkei, Phys. Chem. Earth 100 (2017) 296–304, https://doi.org/10.1016/j.pce.2016.10.001.
[112] A. Pistocchi, G. Cassani, O. Zani, Use of the USPED model for mapping soil erosion and managing best land conservation practices, 1st International Congress on Environmental Modelling and Software, Lugano, 24-27 June 2002, 163-168.
[113] M. Lazzari, D. Gioia, M. Piccarreta, M. Danese, A. Lanorte, Sediment yield and erosion rate estimation in the mountain catchments of the Camastra artificial reservoir (Southern Italy): a comparison between different empirical methods, Catena 127 (2015) 323–339, https://doi.org/10.1016/j.catena.2014.11.021.